Layered superconductors. I. Vortex and fluxon phase transitions

Baruch Horovitz
Department of Physics, Ben-Gurion University, Beer-Sheva 84105, Israel
(Received 30 July 1992)

A system of superconducting layers with spacing d, in-layer penetration depth λ_e and Josephson coupling between neighboring layers J is studied. When $J=0$ the system exhibits a two-dimensional (2D) phase transition of vortex unbinding at a temperature T_v. When $\lambda_e \lesssim d$ a finite-size transition at $T_v^{\text{eff}} > T_v$ distinguishes this system from an XY model. When $J \neq 0$, but vortices are neglected, Josephson fluxon loops lead to a distinct phase transition at $T_f > T_v$ in which a significant second nearest-layer coupling is generated. Competing vortices and fluxon loops lead to a three-dimensional phase transition at T_c, where $T_v < T_c < T_f$. For CuO_2-based superconductors ($\lambda_e \gg d$) T_c is near T_f if $T_c \gtrsim J \gg T_c \exp(-E_c'/T_c)$, where E_c' is a renormalized vortex-core energy; T_c drops to T_v as J is decreased, accounting for data on $YBa_2Cu_3O_7/PrBa_2Cu_3O_7$ superlattices.

I. INTRODUCTION

Phase transitions in layered superconductors are of considerable interest since most of the high-temperature superconductors are layered. The structure[1] of superconductors such as $YBa_2Cu_3O_7$, $Bi_2Sr_2CaCu_2O_x$, and $Tl_2Ba_2CaCu_2O_8$ consists of a CuO_2 bilayer (i.e., two CuO_2 layers separated by ~ 3 Å) which is weakly interacting with the other bilayers, being separated by 12–15 Å. Each bilayer is considered as one conducting layer; in the absence of interlayer coupling, each such layer would exhibit two-dimensional (2D) superconductivity.

The issue of dimensionality in layered superconductors is significant in two aspects: (a) A quantitative aspect : how close is the measured transition temperature T_c to that of uncoupled layers? (b) A fundamental aspect: can a layered three-dimensional (3D) system with weak interlayer coupling exhibit a 2D phase transition with the corresponding critical phenomena?

The significance of interlayer coupling was recently tested by producing $(YBa_2Cu_3O_7)_m(PrBa_2Cu_3O_7)_n$ superlattices,[2–4] i.e., m layers of $YBa_2Cu_3O_7$ unit cells separated by n layers of insulating $PrBa_2Cu_3O_7$. As n increased, T_c was found to decrease, saturating at[3,4] $n=8$–16. In particular, for $m=1$, T_c dropped from 90 K ($n=0$) to ~ 20 K ($n=16$). Disorder or charge depletion may account for some of this reduction; however, this by itself should reduce T_c to zero at large n. The saturation of T_c at large n therefore indicates that the loss of interlayer coupling should be a significant cause for the reduction in T_c. A single $YBa_2Cu_3O_7$ layer[5] has shown a similar resistance curve to that of the 1×16 superlattice, supporting the claim for saturation. Data on $(Bi_2Sr_2CaCu_2O_8)_m(Bi_2Sr_2CuO_6)_n$ have shown a decrease of T_c from 59 K ($n=0$) to ~ 30 K ($m=1$, $n=2$) with $Bi_2Sr_2CuO_6$ being a semiconductor.[6] Similar superlattices[7] showed no change in $T_c=75$ K from $n=0$ to $m=1$, $n=5$; however, $Bi_2Sr_2CuO_6$ in the latter case is a superconductor with $T_c=15$ K and is therefore less effective in decoupling the $Bi_2Sr_2CaCu_2O_8$ layers.

Interlayer coupling can also be controlled by iodine intercalation of $Bi_2Sr_2CaCu_2O_x$; T_c is then reduced by 10 K, although the crystal sheet resistance is hardly affected by the intercalation.[8] This indicates that intralayer properties are not affected, leaving the change in interplane coupling as the main cause for the reduction in T_c.

Superconductivity of an isolated layer is described by a 2D phase transition[9] of the Kosterlitz-Thouless[10] and Berezinskii[11] type. The transition temperature T_v separates a regime of thermally excited vortices from that of bound vortices. The presence of such a transition can be observed in two ways:[9] (i) Resistivity ρ_v of free vortices at $T > T_v$, which is of the form

$$\rho_v \sim \exp\{-2[b(T_c^0 - T)/(T-T_v)]^{1/2}\}, \quad T_c^0 > T > T_v , \tag{1}$$

where b is a constant and T_c^0 is the mean-field transition temperature. (ii) Unbinding of vortices by the current at $T < T_v$, leading to a current- (I) voltage (V) relation of the form

$$V \sim I^{a(T)}, \quad T < T_v . \tag{2}$$

The exponent $a(T)$ jumps from 1 to 3 at T_v, while the extrapolation of $a(T)$ to 1 yields T_c^0.

An increasing number of experiments show the presence of the relations (1) and (2) on a variety of compounds,[12–15] as summarized in Table I of Ref. 16. From the values of T_c, T_c^0, and the London penetration depth, the thickness of a superconducting layer relative to that of a single CuO_2 layer, ℓ_{eff}, can be deduced. This analysis shows that ℓ_{eff} is much less than the number of layers in the samples, though it is 6–14, i.e., larger than 1. These experiments seem contradictory—the nonlinear I-V indicates 2D phenomena of uncoupled layers, while the strong dependence of T_c on layer separation implies strong interlayer coupling.

The theoretical study of layered superconductors is based on the Ginzburg-Landau continuum theory for each layer and a Josephson coupling between neighboring layers.[17–18] This model defines two types of topological excitations: (i) vortices, which are point singularities in each plane, and (ii) fluxons, which are lines parallel to the layers across which the relative phase of neighboring layers changes by 2π.

The system with $J=0$ was first solved by Efetov,[19] and more recently was further studied by several authors.[20–24] It was found that although the planes are coupled via the 3D magnetic field, the vortex-vortex interaction is logarithmic in distance, similar to the case of an isolated layer. A 2D-type phase transition for vortex unbinding at a temperature T_v is then expected; this was confirmed recently by an explicit renormalization-group (RG) study.[25]

When $J\neq 0$, fluctuations of fluxon loops compete with the vortex transition. Assuming that vortices are absent, the system has a phase transition at T_f; at $T>T_f$, fluctuations of fluxon loops destroy the correlation between layers allowing for an independent 2D behavior of each layer, while for $T<T_f$ the layers are correlated resulting in a 3D long-range order. The neglect of vortices is consistent for isolated or widely separated junctions, e.g., junctions on twin boundaries[26] in $YBa_2Cu_3O_7$.

For layered superconductors the separate treatment of T_v and T_f is consistent only if $T_f<T_v$—the interval $T_f<T<T_v$ has then (i) no free vortices (being bound below T_v), which is the assumption in deriving T_f, and (ii) J is renormalized to zero (by thermally excited fluxon loops when $T>T_f$), which is the assumption in deriving T_v. The interval $T_f<T<T_v$ (assuming $T_f<T_v$) is a 2D superconducting phase, consistent with the observed nonlinear I-V relation. This was Friedel's motivation for proposing[27] that $T_f<T_v$. However, Korshunov[28] has studied a discrete-Gaussian version for the free energy of layered superconductors and has found that $T_f>T_v$ for all model parameters. Therefore a 2D regime is absent and the transition temperature T_c is a 3D one.

The dependence of T_c on the anisotropy is essential for understanding the data on the superlattices. For the anisotropic layered X-Y model,[29] it was argued that $T_c-T_v\sim \ln^{-2}(J/T_c)$, while Korshunov[28] has argued that $\ln(T_c-T_v)\sim T_c/J$; both results are for small J/T_c.

A related problem is the full range of T_c/T_v as the system becomes isotropic. Numerical data[30,31] on the X-Y model limits T_c to be in the range $1<T_c/T_v<2.4$, with the upper limit given by the isotropic X-Y model. Experimentally, however, T_c changes by a factor of ~ 4, while the X-Y coupling τ decreases at higher T (e.g., in the mean field $\tau\sim T_c^0-T$); thus, T_c/τ changes by $\sim 4(T_c^0-T_v)/(T_c^0-T_c)$, which is much larger than the 2.4 value of the X-Y model.

The excessive drop of T_c/τ (beyond the 2.4 factor) has been related to a change of T_c^0 due to either boundary effects[30] or to change depletion from the YBCO layers.[32] The latter effect was found to correlate[32] with fits of Eq. (1), which indicate a decrease in T_c^0. Since direct data on intralayer properties of superlattices are not yet available, the experimental value of the allowed range of T_c/τ is not yet settled.

In the present paper, the phase transition in layered superconductors is studied in detail, expanding the presentation of previous publications.[25,33] In particular, I show that the $T_c(J)$ dependence can account for a large variation in T_c, which is due to the presence of a core-energy parameter E_c, a parameter which is absent in the conventional X-Y model.

Section II presents the model and its transformation to vortex and fluxon variables. Section III solves the $J=0$ system, showing the vortex transition T_v and the vortex correlation length ξ_v. Section IV solves the system with $J\neq 0$, but assuming that vortices are not present; this yields the fluxon transition at T_f and a correlation length ξ_f. Section V then shows that the full system, with both vortices and fluxons, scales to a 3D isotropic system when $\xi_v\approx\xi_f$, which therefore defines the 3D transition temperature T_c. Section VI analyzes data on T_c of superlattice systems. In a subsequent paper,[16] the effect of magnetic fields parallel to the layers is studied. It is shown there that such fields may decouple the system into effective 2D layers, accounting for the observed I-V data, even for relatively strong interlayer coupling.

II. MODEL

Consider an infinite stack of parallel layers with spacing d in the z direction; each layer is continuous in the $\mathbf{r}=(x,y)$ plane. A Ginzburg-Landau-type free energy is given in terms of an order parameter $|\psi|\exp[i\varphi_n(\mathbf{r})]$ on the nth layer and the 3D vector potential $\mathbf{A}(\mathbf{r},z)$. For temperatures not too close to the mean-field transition temperature, the dominant fluctuations are due to the phase $\varphi_n(\mathbf{r})$ and the amplitude $|\psi|$ can be taken as a constant except near vortices. A vortex is a singular point on one given layer around which $\varphi_n(\mathbf{r})$ changes by 2π. Each singularity must be accompanied by a reduction of $|\psi|$, which vanishes at the vortex center; the reduction extends over the coherence length ξ_0. The presence of vortices can therefore be defined by an integer field $s_n(\mathbf{r})$, which takes values of $0,\pm 1$ on a lattice of spacing ξ_0. The amplitude variation at each vortex generates a core energy E_c, which is roughly the loss of condensation energy in a volume $\xi_0^2 d_0$, where d_0 is the layer thickness. Note that this core energy is present in addition to the energy of the $\pm 2\pi$ phase winding with a constant $|\psi|$ outside the core.

Each layer is assumed to be sufficiently thin ($d_0<\xi_0$) so that $\varphi_n(\mathbf{r})$ and $\mathbf{A}(\mathbf{r},z)$ are z independent within each layer. The supercurrent energy involves then the coefficient

$$\int dz\,|\psi|^2\sim d_0/\lambda^2\equiv 1/\lambda_e\ ,$$

where λ is the London penetration length parallel to the layers; typically, $\lambda_e\approx 10^6-10^7$ Å $\gg d\approx 10$ Å for the CuO_2 systems. The Lawrence-Doniach effective free energy,[17,18] supplemented with the core-energy term, is therefore

$$\mathcal{F}=\frac{1}{8\pi}\int d^2r\,dz\left\{(\vec{\nabla}\times\vec{A})^2+\frac{1}{\lambda_e}\sum_n\left[\frac{\phi_0}{2\pi}\nabla\varphi_n(\mathbf{r})-\mathbf{A}(\mathbf{r},z)\right]^2\delta(z-nd)\right\}$$

$$-\frac{J}{\xi_0^2}\sum_n\int d^2r\cos\left[\varphi_n(\mathbf{r})-\varphi_{n-1}(\mathbf{r})-(2\pi/\phi_0)\int_{(n-1)d}^{nd}A_z(r,z')dz'\right]+E_c\sum_{\mathbf{r},n}s_n^2(\mathbf{r})\ , \tag{3}$$

where J is the Josephson coupling and $\phi_0=hc/2e$ is the flux quantum; two-component vectors are boldfaced, while three-component ones are arrowed, e.g., $\vec{A}$. The four terms of (3) describe the 3D magnetic energy, the 2D supercurrents, the Josephson coupling, and the vortex-core energy, respectively.

In the limit of charge $e\to 0$ (with $\lambda_e\sim e^{-2}$) and $E_c=0$, Eq. (3) reduces to an anisotropic X-Y model

$$\mathcal{F}_{XY}=\sum_n\int d^2r\left\{\frac{\tau}{8\pi}[\nabla\varphi_n(\mathbf{r})]^2-\frac{J}{\xi_0^2}\cos[\varphi_n(\mathbf{r})-\varphi_{n-1}(\mathbf{r})]\right\}\ , \tag{4}$$

where $\tau=\phi_0^2/4\pi^2\lambda_e$. For slow n dependence, the cosine can be expanded, identifying an anisotropy parameter $8\pi d^2J/\xi_0^2\tau$; when this parameter is ≈ 1, $\mathcal{F}_{XY}$ becomes isotropic.

Returning to the general $e\neq 0$ system of Eq. (3), it is useful to separate the phase into its singular and nonsingular components. This separation yields the natural variables $s_n(\mathbf{r})$ and $\theta_n(\mathbf{r})$ of this system, where

$$\varphi_n(\mathbf{r})=\sum_{\mathbf{r}'}s_n(\mathbf{r}')\alpha(\mathbf{r}-\mathbf{r}')+\varphi_n^0(\mathbf{r})\ , \tag{5a}$$

$$\theta_n(\mathbf{r})=\varphi_n^0(\mathbf{r})-\varphi_{n-1}^0(\mathbf{r})-(2\pi/\phi_0)\int_{(n-1)d}^{nd}A_z(\mathbf{r},z')dz'\ , \tag{5b}$$

with $\alpha(\mathbf{r})=\tan^{-1}(y/x)$ and $\varphi_n^0(\mathbf{r})$ is the nonsingular part of $\varphi_n(\mathbf{r})$.

The problem at hand is to evaluate the partition sum of Eq. (3), i.e., integrate $\exp[-\mathcal{F}/T]$ over all configurations of $\vec{A}(\mathbf{r},z)$, $\theta_n(\mathbf{r})$, and $s_n(\mathbf{r})$. A significant simplification is achieved by first integrating $\vec{A}(\mathbf{r},z)$, which can be done exactly since $\vec{A}(\mathbf{r},z)$ is a Gaussian variable. The procedure is to solve for the minimum condition $\delta\mathcal{F}/\delta\vec{A}(\mathbf{r},z)=0$ for $\vec{A}(\mathbf{r},z)$ in terms of $\theta_n(\mathbf{r})$ and $s_n(\mathbf{r})$ and resubstitute in Eq. (3). This leads to the main result of this section: Eq. (15), an effective free energy in terms of $\theta_n(\mathbf{r})$ and $s_n(\mathbf{r})$, which is exactly equivalent to the original system of Eq. (3).

In fact, A_z is determined by A_x, A_y and the gauge condition, e.g., in the London gauge $\vec{\nabla}\cdot\vec{A}=0$ and $\vec{A}\cdot\vec{n}=0$ on the surface ($\vec{n}$ is normal to the surface). Thus one needs the solution for A_x, A_y from $\delta\mathcal{F}/\delta\,\mathbf{A}(\mathbf{r},z)=0$, i.e.,

$$-\nabla^2\mathbf{A}=\sum_n[\Phi_n(\mathbf{r})-\mathbf{A}(\mathbf{r},z)]\delta(z-nd)/\lambda_e\ , \tag{6}$$

where $\Phi_n(\mathbf{r})=(\phi_0/2\pi)\nabla\varphi_n(r)$. The Fourier transform of $\nabla\alpha(r)$ is $2\pi i\hat{\mathbf{z}}\times\hat{\mathbf{q}}/q$, where $\hat{\mathbf{z}}$ and $\hat{\mathbf{q}}$ are unit vectors in the z and $\mathbf{q}$ directions, respectively; $\mathbf{q}$ and k are Fourier transform variables of $\mathbf{r}$ and n, respectively. Hence the Fourier transform of $\Phi_n(\mathbf{r})$ is, from Eq. (5a),

$$\Phi(\mathbf{q},k)=d\sum_n\int d^2r\,\Phi_n(\mathbf{r})\exp(i\mathbf{q}\cdot\mathbf{r}+iknd)=(i\phi_0/q)\hat{\mathbf{z}}\times\hat{\mathbf{q}}s(\mathbf{q},k)/\xi_0^2-(i\phi_0/2\pi)\mathbf{q}\varphi^0(\mathbf{q},k)\ , \tag{7}$$

where $\varphi^0(\mathbf{q},k)$ and $s(\mathbf{q},k)$ are Fourier transforms of $\varphi_n^0(\mathbf{r})$ and $s_n(\mathbf{r})$, respectively [with $\sum_{\mathbf{r}}\to\int d^2r/\xi_0^2$ in the $s(\mathbf{q},k)$ definition]. Here $|k|<\pi/d$, while $q=|\mathbf{q}|$ is limited by the system size R in the x-y plane and by the cutoff on phase fluctuations, Λ, i.e., $1/R<q<\Lambda$ and $\Lambda\approx 1/\xi_0$. Since $\mathbf{A}(\mathbf{r},z)$ is defined on all z, its Fourier transform $\mathbf{A}(\mathbf{q},k)$ has an unbounded k values, while $\mathbf{A}(\mathbf{r},nd)$, defined at the discrete values $z=nd$, has a Fourier transform [defined as in Eq. (7)] $\tilde{\mathbf{A}}(q,k)$, with $|k|<\pi/d$. Using periodic boundary conditions

$$\tilde{\mathbf{A}}(q,k)=\sum_m\mathbf{A}(\mathbf{q},k+2\pi m/d)\ , \tag{8}$$

with summation on all integers m. The Fourier transform of Eq. (6) and application of Eq. (8) yield

$$\tilde{\mathbf{A}}(\mathbf{q},k)=\Phi(\mathbf{q},k)f(q,k)/[1+f(q,k)]\ , \tag{9a}$$

$$\mathbf{A}(\mathbf{q},k)=\Phi(\mathbf{q},k)/\{\lambda_e d(q^2+k^2)[1+f(q,k)]\}\ , \tag{9b}$$

where

$$f(q,k)=\frac{1}{d\lambda_e}\sum_m\frac{1}{q^2+(k+2\pi m/d)^2}=\frac{1}{2\lambda_e q}\frac{\sinh(qd)}{\cosh(qd)-\cos(kd)}\ . \tag{10}$$

Consider next the magnetic-energy term

$$\int d^2r\,dz(\vec{\nabla}\times\vec{A})^2=-\int d^2r\,dz\,\vec{A}\cdot\nabla^2\vec{A}-\int\vec{A}\cdot(\vec{\nabla}\times\vec{A})\times d\vec{s}\ . \tag{11}$$

The term on the surface $d\vec{s}$ vanishes for zero external fields (with a finite external field, it is canceled by the energy of the external field, which has the same surface term with opposite sign). The bulk term, by using Eq. (6), for the A_x, A_y components yields, for the first two terms of Eq. (3),

$$(8\pi\lambda_e d)^{-1}\int d^2q\, dk(2\pi)^{-3}|\Phi(\mathbf{q},k)|^2/[1+f(q,k)] -(8\pi)^{-1}\int d^2r\, dz\, A_z\nabla^2 A_z \ . \quad (12)$$

A_z is determined by the gauge condition, i.e., $A_z(\mathbf{q},k)=-\mathbf{q}\cdot\mathbf{A}(\mathbf{q},k)/k$, with $\mathbf{A}(\mathbf{q},k)$ given by Eqs. (7) and (9b); note that the vortex term does not contribute to A_z; hence, $A_z(\mathbf{q},k)\sim\varphi^0(\mathbf{q},k)$.

In the following we need integrals with periodic functions $g(k)=g(k+2\pi/d)$ of the form

$$\int_{-\infty}^{\infty} dk\, q^2 g(k)/[k^2(q^2+k^2)] =\int_{-\pi/d}^{\pi/d} dk\, g(k)[f(0,k)-f(q,k)]\lambda_e d \ . \quad (13)$$

In the final form, $\varphi^0(\mathbf{q},k)$ is replaced by $\theta(\mathbf{q},k)$ [Eq. (5b)], which by using the solution for $A_z(\mathbf{q},k)$ and Eq. (13) becomes

$$\theta(\mathbf{q},k)=\varphi^0(\mathbf{q},k)[1-\exp(ikd)][1+f(0,k)]/[1+f(q,k)] \ . \quad (14)$$

Note that the vortex and φ^0 terms in Eq. (7) are orthogonal so that when (7) is substituted in (12) these variables decouple; the only coupling in $\mathcal{F}$ is in the cosine term of (3). Finally, substituting $A_z(\mathbf{q},k)$ in terms of $\varphi^0(\mathbf{q},k)$ and $\mathbf{A}(\mathbf{q},k)$ in terms of $s(q,k)$ and $\varphi^0(\mathbf{q},k)$ in Eq. (12), using Eqs. (13) and (14), yields for the effective free energy with $\vec{A}$ being integrated out,

$$\mathcal{F}'=\tfrac{1}{2}T\sum_{n,\mathbf{r};n',\mathbf{r}'} s_n(\mathbf{r})G_v(\mathbf{r}-\mathbf{r}',n-n')s_{n'}(\mathbf{r}')+E_c\sum_{n,\mathbf{r}} s_n^2(\mathbf{r})+\tfrac{1}{2}T\sum_{\mathbf{q},k} G_f^{-1}(\mathbf{q},k)|\theta(\mathbf{q},k)|^2 -(J/\xi_0^2)\sum_n\int d^2r\cos\left\{\theta_n(\mathbf{r})+\sum_{\mathbf{r}'}[s_n(\mathbf{r}')-s_{n-1}(\mathbf{r}')]\alpha(\mathbf{r}-\mathbf{r}')\right\} , \quad (15)$$

where

$$G_v(\mathbf{q},k)=\pi d(\tau/T)\{[1+f(\mathbf{q},k)]q^2\}^{-1} , \quad (16a)$$

$$G_f(\mathbf{q},k)=4\pi(T/\tau)(d^2/\lambda_e)[1+(4\lambda_e/d)\sin^2(kd/2)]/q^2 , \quad (16b)$$

and $\tau=\phi_0^2/(4\pi^2\lambda_e)$. As an additional check, Eq. (15) was rederived in the axial gauge ($A_z=0$), confirming that it is gauge invariant.

The terms of Eq. (15) represent the vortex-vortex interaction, the vortex-core energy, the deformation energy of the nonsingular phase $\theta_n(\mathbf{r})$, and the Josephson coupling, respectively. Note that the Josephson term is the only one which couples the variables $\theta_n(\mathbf{r})$ and $s_n(\mathbf{r})$.

The next two sections analyze two limits of the free energy (15), while Sec. IV returns to study the full problem of Eq. (15).

III. VORTEX TRANSITION

In this section the system with $J=0$ is studied. The well-known logarithmic interaction[19–25] between vortices is first reproduced, and then a RG analysis is presented.

The Fourier transform of Eq. (16a) yields the vortex-vortex interaction in real space,

$$G_v(r,n)=\frac{\tau}{2T}\int_{1/R}^{\Lambda}\frac{dq}{q}J_0(qr)\left\{\delta_{n,0}-\frac{\sinh(qd)}{2\lambda_e q}[b^{-2}(q)-1]^{-1/2}\{b^{-1}(q)-[b^{-2}(q)-1]^{1/2}\}^{|n|}\right\} , \quad (17)$$

where $J_0(qr)$ is a Bessel function of the first kind and

$$b(q)=\frac{2\lambda_e q}{2\lambda_e q\cosh(qd)+\sinh(qd)} \ . \quad (18)$$

The long-range behavior of (17) is obtained for $r\gg d$, where $b(q)$ can be approximated by $b(0)=2\lambda_e/(2\lambda_e+d)$; hence,

$$G_v(r,n)=-\frac{\tau}{2T}\left\{\delta_{n,0}-\left[1+\frac{4\lambda_e}{d}\right]^{-1/2}\left[1+\frac{d}{2\lambda_e}-\left[\frac{d}{\lambda_e}+\frac{d^2}{4\lambda_e^2}\right]^{1/2}\right]^{|n|}\right\}\ln(r/R) \ . \quad (19)$$

In particular, for $d\ll\lambda_e$, as for the Cu_2O layers,

$$G_v(r,n)=-(\tau/2T)\ln(r/R)\ ,\quad n=0\ , \tag{20a}$$

$$G_v(r,n)=(\tau/4T)(d/\lambda_e)^{1/2}\exp[-|n|(d/\lambda_e)^{1/2}]\ln(r/R)\ ,\quad n\neq 0\ . \tag{20b}$$

The logarithmic interaction between vortices on different layers is much weaker than for those on the same layer. Note also that the exponential factor has a long decay length of $(\lambda_e/d)^{1/2}$ layers.

The usual Kosterlitz-Thouless[10] argument leads now to a free energy of a single vortex,

$$\tfrac{1}{2}TG_v(\xi_0,0)-T\ln(R/\xi_0)^2=2(T_v-T)\ln R+\text{const}\ .$$

for large R, where the vortex transition temperature from Eq. (19) is

$$T_v=\frac{\tau}{8}[1-(1+4\lambda_e/d)^{-1/2}]\ . \tag{21}$$

For $T>T_v$, creation of free vortices is favored, leading to a finite vortex density, while for $T<T_v$ the vortex density vanishes. This argument is presented in more detail in Appendix B and an effective free energy is derived.

It is instructive to consider also the shorter-range behavior of $G_v(r,n)$. When $d\ll\lambda_e$, $G_v(r,n)$ is logarithmic at both large distance [Eq. (20)] and short distance $r\ll d$, e.g., $G_v(r,0)=-(\tau/2T)\ln(r/R)$. The situation is more interesting when $d\gg\lambda_e$:

$$G_v(r,0)=-(\tau\lambda_e/Td)\ln r/R,\quad \lambda_e\ll d\ll r\ , \tag{22a}$$

$$G_v(r,0)=(\tau\lambda_e/Tr)+\text{const},\quad \lambda_e\ll r\ll d\ , \tag{22b}$$

$$G_v(r,0)=-(\tau/2T)\ln(r/R),\quad r\ll\lambda_e\ll d\ , \tag{22c}$$

so that the interaction is not logarithmic only in the intermediate range of $\lambda_e\ll r\ll d$. Note also that the coefficients of the logarithmic interaction vary from $\tau/2T$ at short distance to $\tau\lambda_e/Td$ at very long distance.

Before presenting the RG analysis, it is useful to consider some magnetic properties of vortices. The single-vortex configuration has a magnetic field which penetrates through neighboring layers on which the phase is nonsingular. The usual scenario of flux penetration into a superconductor, e.g., in the 3D case, involves currents $\vec{J}=(c/4\pi)\vec{\nabla}\times\vec{\nabla}\times\vec{A}$, which decay faster than $1/r$. Integration of the London equation [Eq. (6)] along a circle of large radius yields then flux quantization and that a finite flux must be related to an integer number of vortices. However, in layered superconductors (with coupling $J=0$), the currents decay as $1/r$; in fact, the current due to a single vortex at the origin is in the azimuthal direction $\hat{\theta}$, with magnitude

$$J_\theta(r,z)=-(cT/\phi_0)\sum_n\frac{\partial}{\partial r}G_v(r,n)\delta(z-nd)\ . \tag{23}$$

This can be derived either directly from Eq. (9) or by noting that this current represents the Lorenz force of one vortex on another one and is therefore proportional to the gradient of the vortex-vortex potential $TG_v(r,n)$. The logarithmic form of $G_v(r,n)$ leads then to currents which decay as $1/r$; thus, the current term can balance the flux term in Eq. (6) without a phase singularity.

The coefficient of the $1/r$ term in Eq. (23) determines the total flux (in the z direction) through the nth layer due to a vortex at the 0th layer:

$$\phi(n)=\phi_0\left[1+\frac{4\lambda_e}{d}\right]^{-1/2}\left[1+\frac{d}{2\lambda_e}-\left[\frac{d}{\lambda_e}+\frac{d^2}{4\lambda_e^2}\right]^{1/2}\right]^{|n|}\ . \tag{24}$$

In particular, the flux $\phi(0)$ through the plane with the vortex can be much smaller than ϕ_0 if $\lambda_e\gg d$. The flux acquires a radial component at $z\neq 0$ reducing its z component; $\phi(n)$ vanishes for $n\to\infty$ so that at large distances the whole flux escapes in the radial direction.

An important question is whether a single vortex is the lowest-energy excitation—it might be favorable for a single vortex to nucleate other ones so as to reduce the long-range currents. Consider a vortex "line" of length m consisting of m point vortices, one on top of the other, i.e., on planes $n=0,1,\dots,m-1$ at $r=0$. The corresponding energy, for $\lambda_e\gg d$, is

$$\begin{aligned}E(m)&=\tfrac{1}{2}\sum_{n,n'=0}^{m-1}TG_v(0,n-n')+mE_c\\&=(\tau/8)\{m\ln(d\lambda_e/\xi_0^2)+2\sqrt{\lambda_e/d}\\&\qquad\times[1-\exp(-m\sqrt{d/\lambda_e})]\ln R\}+mE_c+C\ ,\end{aligned} \tag{25}$$

where C is independent of m (or of R) in the limit $m\to\infty$ (or $R\to\infty$), respectively. Thus $E(m)$ is an increasing function of m and $m=1$ is the lowest-energy excitation. In particular, the $\ln R$ term is canceled when $m\gg(\lambda_e/d)^{1/2}$; similar conclusions apply to all λ_e/d. The cancellation of the $\ln R$ term is related to the $q,k\to 0$ form of

$$G_v(q,k)\sim\{q^2+q^2/[\lambda_e d(q^2+k^2)]\}^{-1}\ ,$$

which is nonsingular when $k=0$.

The total magnetization of a single vortex is in the z direction, with the rather simple result

$$M_z=\int(\vec{\nabla}\times\vec{A})_z d^3r=\phi_0 d\ . \tag{26}$$

An external magnetic field $H^\perp$ perpendicular to the layers couples to m vortices with the energy $H^\perp m\phi_0 d/4\pi$. The lowest field at which this energy overcomes the creation energy (25) is for $m\to\infty$ and is given by (at $T=0$ and $\lambda_e\gg d$)

$$H_{c1}^\perp=\phi_0[\tfrac{1}{2}\ln(\lambda_e d/\xi_0^2)+4E_c/\tau]/(4\pi\lambda_e d)\ . \tag{27}$$

The usual 3D form of $H_{c1}^\perp$ is obtained by using an effective London penetration length $\lambda_{ab}=(\lambda_e d)^{1/2}=\lambda(d/d_0)^{1/2}$, i.e., as if the condensate density $\sim\lambda^{-2}$ is spread over the whole spacing d, reducing the average condensate density by factor d_0/d.

The case of an isolated layer[34] is obtained in the limit $d\to\infty$, i.e., $\phi(0)=\phi_0$ [Eq. (24)], while $M_z\to\infty$ and $H_{c1}^{\perp}\to 0$. Note also that the vortex-vortex interaction in an isolated layer is not logarithmic at very large distances [Eq. (22b)], while with a finite d screening from other layers always result in logarithmic interaction for $r \gg d$.

I proceed now to study the finite-temperature behavior by applying the RG method. The partition function Z of (15) with $J=0$ is first transformed into that of a sine-Gordon system by rewriting it as

$$Z=\int \mathcal{D}\chi \exp\left[-\tfrac{1}{2}(2\pi)^{-3}\int d^2q\, dk G_v^{-1}(q,k)|\tilde{\chi}(\mathbf{q},k)|^2 - i\sum_{n,\mathbf{r}}\tilde{\chi}_n(\mathbf{r})s_n(\mathbf{r}) - (E_c/T)\sum_{n,\mathbf{r}} s_n^2(\mathbf{r})\right] . \tag{28}$$

When the Gaussian field $\tilde{\chi}_n(\mathbf{r})$ is integrated, the original form (15) is recovered. Instead, the sum on $s_n=0,\pm 1$ can be performed at each site $\mathbf{r}$ leading to a factor of

$$\prod_{\mathbf{r}}[1+y_0\cos\tilde{\chi}_n(\mathbf{r})]\approx \exp\left[y_0\sum_{n,\mathbf{r}}\cos\tilde{\chi}_n(\mathbf{r})\right] , \tag{29}$$

where $y_0=2\exp(-E_c/T)$ and a $y_0^2\cos 2\tilde{\chi}_n(\mathbf{r})$ term, being irrelevant near the phase transition, is neglected. Since E_c is a chemical potential for vortices, y_0 is known as the vortex fugacity.

The resulting free energy has the form of the sine-Gordon system [Eq. (A1)], and the RG procedure, as detailed in Appendix A, can be followed. Equation (A4) identifies the function

$$g(q,k)=(\tau/8T)[1+f(q,k)]^{-1} . \tag{30}$$

To check the relevancy of $\cos[\tilde{\chi}_n(\mathbf{r})\pm\tilde{\chi}_{n'}(\mathbf{r})]$, consider Eq. (A18) for $X_n(h_0=h_1=0)=(\tau/8T)\{\cdots\}$, where $\{\cdots\}$ are the brackets in Eq. (17). It can be checked that $X_{n\neq 0}\ll X_0$ near $X_0=1$ [see, e.g., Eq. (20)] so that all these terms, including the v and h_1 terms in (A1) and (A4), can be neglected. The recursion relations (A20) therefore involve only the fugacity y and the self-energies of type h_0:

$$\begin{aligned} dy&=2y[1-X_0(h_0,1/\xi)]d\ln\xi ,\\ dh_0&=2\gamma^2y^2X_0(h_0,1/\xi)d\ln\xi , \end{aligned} \tag{31}$$

with initial conditions $y(\xi_0)=y_0$, $h_0(\xi_0)=0$, and $X_0=X_0(h_0,q)$,

$$X_0(h_0,q)=\{h_0+8T/\tau\}^{-1}\left[1-\sinh(qd)\{[2\lambda_e(1+h_0\tau/8T)q\cosh(qd)+\sinh(qd)]^2-[2\lambda_e(1+h_0\tau/8T)q]^2\}^{-1/2}\right] . \tag{32}$$

To first order in y, the transition temperature of (31) is determined by $X_0(h_0=0,1/\xi=0)$ and Eq. (21) is recovered precisely. The phase transition is now interpreted according to the flow of the vortex fugacity y; for $T<T_v$, y flows to zero and vortices are absent on long scales, while, for $T>T_v$, y flows to a finite value; i.e., vortices are thermally excited.

To second order in y and for $\lambda_e/d\gg 1$, as typical for CuO_2-based superconductors, $X_0=(h_0+8T/\tau)^{-1}$; considering X_0 as the scaling variable instead of h_0, Eq. (31) reduces to the standard 2D scaling[10,11]

$$dy=2y(1-X_0)d\ln\xi , \tag{33a}$$

$$dX_0=-2\gamma^2y^2X_0^3 d\ln\xi , \tag{33b}$$

with the initial values $y(\xi_0)=y_0$, $X_0(\xi_0)=\tau/8T$. The trajectories of (33) are the well-known hyperbolas[10,11,35–37] of the form

$$\left[\frac{1}{X_0}-1\right]^2-\gamma^2y^2=\left[\frac{8T}{\tau}-1\right]^2-\gamma^2y_0^2\equiv A , \tag{34}$$

with a phase transition at

$$T_v=(\tau/8)(1-\gamma y_0) . \tag{35}$$

For $T>T_v$, y is relevant and reaches a strong-coupling situation $y\approx 1$, where thermal fluctuations are inefficient. Thus ξ_v for which $y(\xi_v)\approx 1$ is identified as the vortex correlation length. Near T_v [i.e., $A<0$, $T_v<T<(\tau/8)(1+\gamma y_0)$], y first decreases and then increases to $y\approx 1$ at the scale

$$\begin{aligned}\xi_v&\approx\xi_0\exp[\pi/4(-A)^{1/2}]\\ &=\xi_0\exp[(\pi^2/32\gamma y_0)(1-T/T_c^0)/(T/T_v-1)]^{1/2} ,\end{aligned} \tag{36}$$

where the form $\tau=\tau_0(1-T/T_c^0)$ has been used. For $T>T_v$, but not too close to $T_v[T\gtrsim(\tau/8)(1+\gamma y_0)]$, the effect of the second-order term in y is not significant, leading to

$$\xi_v\approx\xi_0[y_0]^{-(2-\tau/4T)^{-1}} . \tag{37}$$

These results are confirmed by numerical solutions of the full equations for $\lambda_e/d=10^3$ as shown in Fig. 1(a). Since the self-energy h_0 is mainly effective in the combination h_0+8T/τ, the latter can be interpreted as a temperature renormalization.

It is interesting to consider the case of $d\gtrsim\lambda_e$, which applies to isolated or well-separated 2D junctions, e.g., junctions on twin boundaries[21] in $YBa_2Cu_3O_7$. For scales $\xi\ll\lambda_e$, $X_0\approx\tau/8T$ (for small h_0) and the scaling (31) acts as if $T_v=\tau/8$, while, in the final integration range $\xi\gg d$,

$X_0 \approx \lambda_e \tau / 4dT$ and scaling proceeds as appropriate for the thermodynamic limit transition $T_v = \lambda_e \tau / 4d \lesssim \tau/8$. Thus, for $\lambda_e \tau / 4d \lesssim T \lesssim \tau/8$, $y(\xi)$ first decreases, as if the system were ordered, but eventually $y(\xi)$ increases when $\xi > \lambda_e$ to signal the actual disordered phase. It is possible, however, that the latter increase is smaller than the former decrease because of a finite size R. This defines a finite-size transition temperature T_v^{eff}, which can be much higher than T_v if $d \gg \lambda_e$,

$$T_v^{\text{eff}} = (\tau/8)\ln(2\lambda_e/\xi_0)/\ln(R/\xi_0) + O(y_0)\ , \quad R \gg \lambda_e\ , \tag{38a}$$

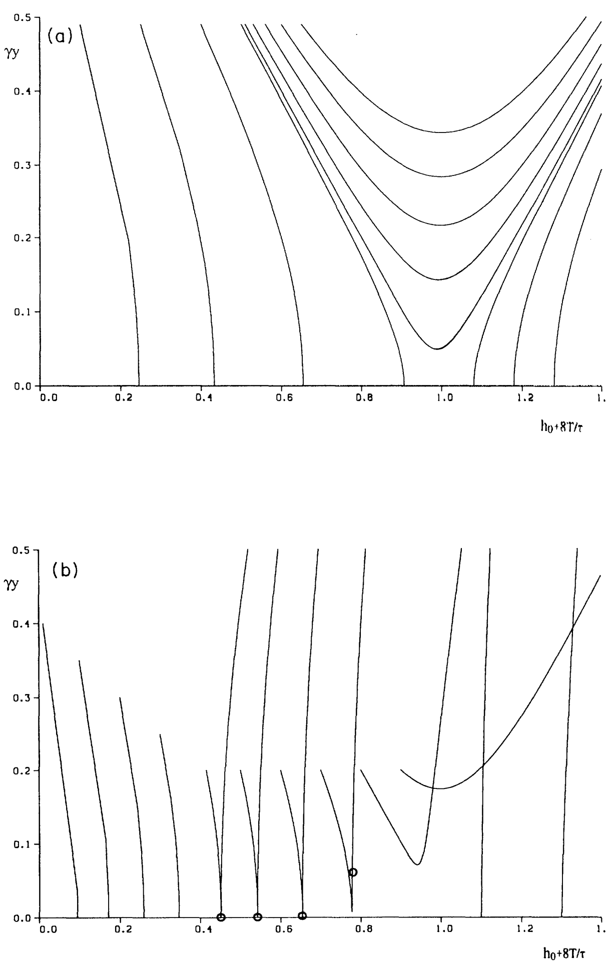

FIG. 1. Scaling of the vortex system [Eqs. (31) and (32)] for vortex fugacity y and self-energy h_0 [the axis is $h_0 + T/\tau$, which may be interpreted as a renormalized temperature; γ is a nonuniversal parameter, see Eq. (A7)]. Trajectories start on their left end with various $8T/\tau$ and initial $y(\xi_0)$ values, as can be inferred from the figure. (a) $\lambda_e/d = 10^3$ and $\lambda_e/\xi_0 = 10^3$. (b) $\lambda_e/d = 0.1$ and $\lambda_e/\xi_0 = 10^3$. The marked circles in case (b) correspond to the point where ξ reaches $10^4 \xi_0$.

$$T_v^{\text{eff}} = \tau/8 + O(y_0), \quad R \ll \lambda_e\ . \tag{38b}$$

The result (38) is confirmed by numerical solution of the full equations (31) for $\lambda_e/d = 0.1$ and $\lambda_e/\xi_0 = 10^3$ [Fig. 1(b)]. The strict phase transition is, for $\gamma y_0 = 0.2$, at $T/8\tau = 0.415$; however, for a system size $R = 10^4 \xi_0$, the renormalized γy at $\xi = R$ is reached at the points marked by the circles in Fig. 1(b). These points correspond to $\gamma y > 0.2$ only for $T/8\tau \gtrsim 0.8$, i.e., $T_v^{\text{eff}}/8\tau \approx 0.8$.

Note that the existence of T_v^{eff} is due to the gauge coupling e; for the corresponding X-Y model ($e \to 0$ and $\lambda_e \sim e^{-2} \to \infty$), the condition $d \gtrsim \lambda_e$ for Eq. (38) cannot apply. Consider two interesting limiting examples where the effect of $e \neq 0$ is significant: first, the well-known case of an isolated superconducting film,[9] i.e., $d \to \infty$. Unlike the X-Y system, there is no strict phase transition in this case ($T_v \sim d^{-1} \to 0$) and just the finite-size transition (38) survives. This is due to the screening of the vortex singularity beyond the distance λ_e, a screening which is absent in an X-Y model. The second example is the case of thick layers, i.e., a system of bulk superconductors joined by 2D junction (*both* d and d_0 become large). Note, however, that our starting model is valid only if d_0 is not too large; i.e., $\tau/8$ should not be too close to T_c^0 so that the 3D correlation is still short, i.e., $\xi_{3\text{D}} < d_0$. Thus increasing $d \to \infty$ and $d_0 \to \xi_{3\text{D}}$ implies that $T_v \to 0$, while $T_v^{\text{eff}} \to T_c^0$; the latter is the correct T_c, since the layer is becoming a bulk system.

IV. FLUXON TRANSITION

In this section Eq. (15) is studied in the limit of absent vortices; i.e., the only allowed configuration for $s_n(\mathbf{r})$ is $s_n(\mathbf{r}) = 0$; this limit can be considered as the $E_c \to \infty$ limit of Eq. (15). As shown in Sec. V, the resulting phase transition is an upper bound for the actual finite E_c transition temperature T_c and its correlation length is involved in determining T_c.

The topological excitations in this system are due to the $J\cos\theta_n(\mathbf{r})$ term of the free energy. These excitations are lines in between neighboring layers, so that by crossing these lines in the x,y plane the relative phase of the layers [$\theta_n(\mathbf{r})$ of Eq. (5b)] changes by $\pm 2\pi$. These lines are known as Josephson vortices or fluxons, and the latter terminology is adopted here. Unlike vortices (those of Sec. III), fluxons do not have a singular core since the fluxon line is in between superconducting layers. Thermal fluctuations are expected to generate fluxon loops between neighboring layers—inside a loop, $\theta_n(\mathbf{r})$ is $\pm 2\pi$ different from $\theta_n(\mathbf{r})$ outside the loop. Crossing the loop, $\theta_n(\mathbf{r})$ varies smoothly over a finite length.

The magnetization of a fluxon, unlike its core, is not confined to a single interlayer spacing. Using Eqs. (7), (9b), and (13), the magnetization in the x direction can be written as

$$M_x(\mathbf{r},n)=\int_{(n-1)d}^{nd} dz(\vec{\nabla}\times\vec{A})_x$$
$$=-(\phi_0/2\pi)d\int dk/2\pi\sum_{n'}[1+(4\lambda_e/d)\sin^2\tfrac{1}{2}kd]^{-1}[\partial\theta_{n'}(\mathbf{r})/\partial y]\exp[ik(n-n')d]\ . \tag{39}$$

Similarly $M_y(\mathbf{r},n)$ involves $\partial\theta_{n'}(\mathbf{r})/\partial x$, while $M_z(\mathbf{r},n)=0$. For a single fluxon line, $\int dy\,\partial\theta_{n'}(\mathbf{r})/\partial y=\mp 2\pi$, so that the flux in the x direction turns out to be $\phi_x(n)=\pm\phi(n)$ of Eq. (24). Thus, for $\lambda_e/d\gg 1$, $\phi_x(0)\ll 1$ and $\phi_x(n)$ decays as $\exp[-|n|(d/\lambda_e)^{1/2}]$. Quantization does apply to the total flux, i.e., $\sum_n\phi_x(n)=\pm\phi_0$.

The fluxon system can be solved by the RG procedure of Appendix A. Identify $G(q,k)=G_f(q,k)$ [Eq. (16b)] and $g(q,k)$ of Eq. (A4) as

$$g(q,k)=(Td/2\lambda_e\tau)[1+(4\lambda_e/d)\sin^2\tfrac{1}{2}kd]\ . \tag{40}$$

The variables X_n of Eq. (A18) become, now,

$$X_n(h_0,h_1)=d\int\frac{dk}{2\pi}\frac{(1+d/2\lambda_e-\cos kd)\cos mkd}{\tau/T+(h_0+h_1\cos kd)(1+d/2\lambda_e-\cos kd)}\ . \tag{41}$$

In particular,

$$X_n(0,0)=(T/\tau)[(1+d/2\lambda_e)\delta_{n,0}-\tfrac{1}{2}\delta_{n,\pm 1}]\ . \tag{42}$$

For $n\neq 0,\pm 1$ terms such as $\cos[\tilde{\chi}_0(\mathbf{r})\pm\tilde{\chi}_n(\mathbf{r})]$ are irrelevant since for these $X_n(0,0)=0$ [see condition of Eq. (A23)]. However, for $n=\pm 1$, $X_\pm=-\frac{1}{2}(1+d/2\lambda_e)$ when $X_0=1$; i.e., for $d/\lambda_e\ll 1$, the free-energy term $v\cos[\tilde{\chi}_n(\mathbf{r})+\tilde{\chi}_{n+1}(\mathbf{r})]$ is almost relevant at $X_0=1$. In other words, y and v become relevant (in first order) at a small parameter difference $|X_0-X_{\pm 1}|\approx d/\lambda_e\ll 1$, so that one cannot neglect the v term in the RG procedure. In terms of the original phases $\varphi_n(\mathbf{r})$, the v term corresponds to a Josephson coupling between next-nearest layers.

The RG scaling equations are given by Eq. (A20), with X_0, X_1 of Eq. (41) and with initial values at $\xi=\xi_0$ given by $y=J/T$, $v\ll J/T$, $h_0=h_1=0$. Before presenting numerical solutions, it is instructive to consider two simpler limiting situations. First, neglect v and h_1, corresponding to d/λ_e being not too small. Assuming also $h_0\ll 1$,

$$X_0(h_0)=(T/\tau)(1+d/2\lambda_e)-h_0(T/\tau)^2(\tfrac{3}{2}+d/\lambda_e+d^2/4\lambda_e^2)\ . \tag{43}$$

Considering now X_0 as a scaling variable instead of h_0, the RG equations (A20) for y and h_0 become

$$dy=2y(1-X_0)d\ln\xi\ ,\qquad dX_0=-2\tilde{\gamma}^2\tilde{J}^2X_0^3 d\ln\xi\ , \tag{44}$$

where

$$\tilde{\gamma}^2=\gamma^2[\tfrac{3}{2}+d/\lambda_e+d^2/4\lambda_e^2](1+d/2\lambda_e)^{-2}\ ;$$

the initial values are $y_0=J/T$ and $X_0(\xi_0)=(T/\tau)(1+d/2\lambda_e)$. Equation (44) has the standard 2D scaling form[10,11,35–37] identical to that of Eq. (33). The phase transition is at

$$T_f=\tau/[(1+d/2\lambda_e)(1-\tilde{\gamma}J/T]\ . \tag{45}$$

For $T>T_f$, y is irrelevant—i.e., the layers are decoupled by thermally excited fluxon loops—while for $T<T_f$, y is relevant, allowing for full 3D correlations between the layers. Thus T_f is a transition from a phase with 2D power-law corrections at high temperatures to a 3D phase with exponential correlations at low temperatures.

The correlation lengths can be analyzed as done below Eq. (34); near T_f [$\tau/(1+\tilde{\gamma}y_0)<T<T_f$],

$$\xi_f\approx\xi_0\exp[(\pi^2T/32\tilde{\gamma}J)(\tau/T-1+\tilde{\gamma}J/T)^{-1}]^{1/2}$$
$$\approx\xi_0\exp[(\pi^2T^2/32\tilde{\gamma}J\tau_0)(1-T/T_f)^{-1}]^{1/2}\ , \tag{46}$$

where in the last form $\tau=\tau_0(1-T/T_c^0)$ was used. When T is not too close to T_f, $T\lesssim\tau/(1+\tilde{\gamma}y_0)$,

$$\xi_f'\approx\xi_0\left[\frac{J}{T}\right]^{-[2(1-T/\tau)]^{-1}}\ . \tag{47}$$

Consider now a second simplified situation in which both y and v are maintained, but h_0, h_1 are neglected. In particular, in the limit $d/\lambda_e\ll 1$, $X_0=T/\tau$, $X_1=-T/2\tau$, and Eq. (A20) yields

$$dy=[2y(1-T/\tau)+\gamma' yvT/\tau]d\ln\xi\ ,\qquad dv=[2v(1-T/\tau)+\tfrac{1}{4}\gamma' y^2T/\tau]d\ln\xi\ . \tag{48}$$

These equations have the fixed point $y=v=0$, as well as the nontrivial fixed point

$$y^*=\pm(4/\gamma')(1-\tau/T)\ ,\qquad v^*=(2/\gamma')(1-\tau/T)\ , \tag{49}$$

which defines a critical line $v^*=\frac{1}{2}|y^*|\mathrm{sgn}(1-\tau/T)$. Linearizing $(y-y^*,v-v^*)$ near the fixed point yields the eigenvalues

$$\lambda_1=(\xi/\xi_0)^{4(1-T/\tau)}\ ,\qquad \lambda_2=(\xi/\xi_0)^{-2(1-T/\tau)}\ , \tag{50}$$

with eigenvectors $\mathbf{e}_1=(1,\mp 1)$, $\mathbf{e}_2=(1,\pm\frac{1}{2})$ (Fig. 2). For $T>\tau$, e_2 is the relevant direction, while e_1 is irrelevant. For an initial $v=0$, the critical point is at $y_0^c=(6/\gamma')(1-\tau/T)$; i.e., the transition temperature is at

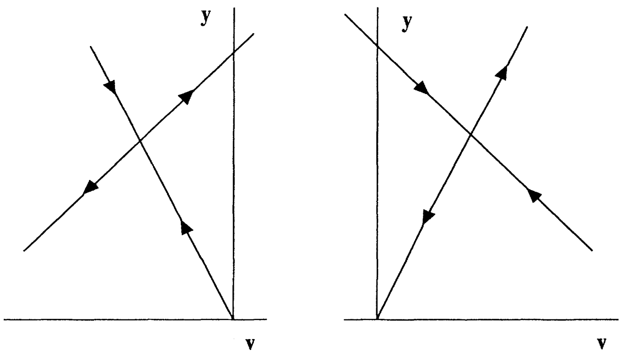

FIG. 2. Structure of the fixed points for the simplified fluxon system [Eq. (48)]: (a) $T<\tau$ and (b) $T>\tau$.

$$T_f=\tau/(1-\gamma' y_0/6)\ , \tag{51}$$

with a correlation exponent $[2(T/\tau-1)]^{-1}$. For $J/T<y_0^c$, $y=v=0$ is the final fixed point which then dominates the critical behavior [Fig. 2(b)]. Comparison of Eq. (51) with Eq. (45) shows that T_f is enhanced by generating either a v term or an h_0 term in a similar way.

For $T<\tau$, $\mathbf{e}_1$ is relevant, while $\mathbf{e}_2$ is irrelevant [Fig. 2(a)]. To reach the fixed point (49), one needs an initial (possibly small) $v(\xi_0)<0$ and the critical y_0 is near zero; the corresponding correlation length is

$$\xi_f''\approx\xi_0\left[\frac{J}{T}\right]^{-[4(1-T/\tau)]^{-1}} . \tag{52}$$

Comparison with Eq. (47) shows that $\xi_f''\ll\xi_f'$; i.e., the vicinity of the fixed point (49) is reached much faster then the vicinity of $y\approx 1$ as defined by ξ_f. Thus the combined effect of y and v enhances the renormalization rate and one may expect that the solution of the RG equation (A20) will show that v is generated and that the final strong-coupling situation is reached faster than the scale of (47); a reasonable guess is that $y\approx 1$ is reached when the correlation length is in between those of Eqs. (47) and (52),

$$\xi_f\approx\xi_0\left[\frac{J}{T}\right]^{-[2\eta(1-T/\tau)]^{-1}} , \tag{53}$$

with $1<\eta<2$, depending on T/τ. The following numerical solutions yield $\eta\approx 1$ at $T/\tau<0.4$ and increasing to 1.4 at $T/\tau=0.9$ when $\tilde{\gamma}J/T=0.01$ or to 1.9 at $T/\tau=0.9$ when $\tilde{\gamma}J/T=0.1$. The increase is, however, mainly due to the h_0 renormalization, with a smaller part due to the generated v term.

Numerical solutions of the full RG equations (A20) with X_0, X_1 given by Eq. (41) are shown in Figs. 3 and 4. Figures 3(a) and 3(b) show a case with $T<\tau$ which is affected by a fixed point with $v^*<0$ similar to that of Fig. 2(a); the trajectory is somewhat dependent on the initial sign of v. For both signs of initial v, the final stage of $y\approx 1$ is accompanied by a fairly large v. Figure 3(c) shows a case with $T>\tau$, affected by a fixed point with $v^*>0$, similar to that of Fig. 2(b); for $T<T_f$, a strong v is again generated. Thus a strong Josephson coupling between next-nearest-neighbor layers is generated when $T<T_f$. This provides an experimental signature which

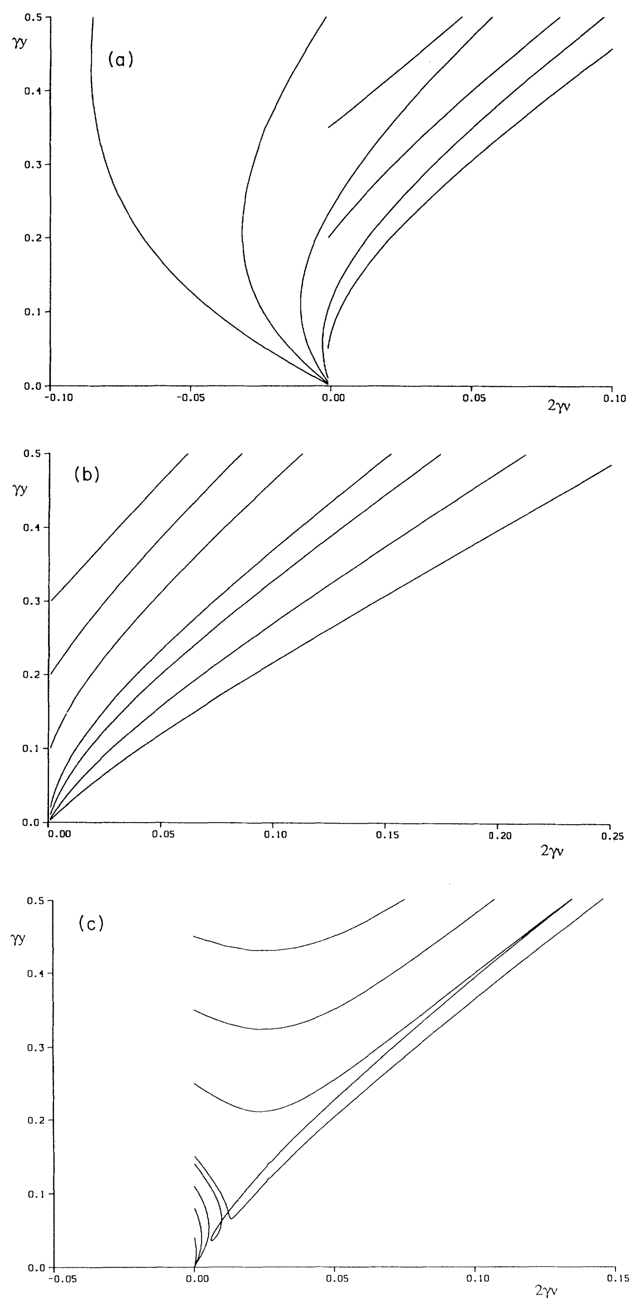

FIG. 3. Scaling of the fluxon system [Eqs. (A20) and (41)] for $\lambda_e/d=10^6$, projected in the y,v plane; y and v are the nearest- and next-nearest-interlayer Josephson couplings [$\gamma=\gamma'$ is assumed, see Eq. (A7)]. The trajectories start near $v=0$ with various initial values $y(\xi_0)$, as can be inferred from the figure (a) $T/\tau=0.8$, $v(\xi_0)=-0.001$. (b) $T/\tau=0.8$, $v(\xi_0)=0.001$. (c) $T/\tau=1.2$, $v(\xi_0)=0$. The choice $v(\xi_0)=\pm 0.001$ has a minor effect on the latter trajectories.

can test the dominance of the fluxon description.

Figure 4 shows the trajectories in the plane of y and $T/(\tau+Th_0)$: the latter combination contains the main effect of the self-energy h_0, which can therefore be interpreted as a temperature renormalization. The other self-energy is usually limited to $h_1<0.01$ with no significant effects. Figure 4(a) is similar in general structure to that of the vortex system [Fig. 1(a)], except that the effective temperature is now renormalized in the opposite direction; this is the usual scenario in systems related by a duality transformation of the form (28). The critical y in Fig. 4(a) is $\gamma y_0=0.136$ for $T/\tau=1.2$ and $\gamma y_0=0.4555$ for $T/\tau=2.2$, which remarkably is within 2% of the critical γy_0 in the absence of the v term [Eq. (45)]. Thus the v term does not enhance T_f; in fact, when $T>T_f$, a small v which is initially generated [Fig. 3(c)] is eventually flowing to $v=0$ so that T_f is weakly affected.

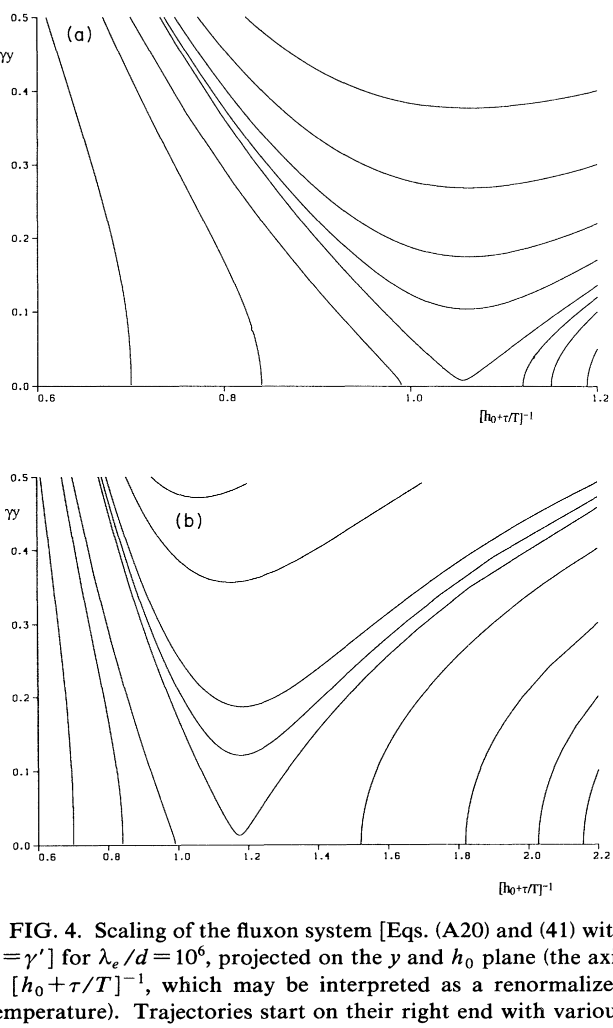

FIG. 4. Scaling of the fluxon system [Eqs. (A20) and (41) with $\gamma=\gamma'$] for $\lambda_e/d=10^6$, projected on the y and h_0 plane (the axis is $[h_0+\tau/T]^{-1}$, which may be interpreted as a renormalized temperature). Trajectories start on their right end with various T/τ and $y(\xi_0)$, as can be inferred from the figure; $v(\xi_0)=0$. The critical y_0^c, defining the phase transition, corresponds to the curve with the sharp minimum. (a) Most of the trajectories have $T/\tau=1.2$, for which $y_0^c=0.136$. (b) Most of the trajectories have $T/\tau=2.2$, for which $y_0^c=0.4555$.

V. VORTEX-FLUXON COMPETITION

I now come to grips with the 3D problem of Eq. (15), where progress can be made based on the insight gained by the vortex and fluxon phase transitions.

The separate treatments of vortices and fluxons in Secs. III and IV would have been consistent if T_f were lower than T_v. In an interval $T_f<T<T_v$, if it existed, the vortex fugacity *and also* the Josephson coupling would be irrelevant so that both descriptions of T_v with $J=0$ (at $T<T_f$) and T_f with no vortices (at $T>T_v$) would be self-consistent. The interval $T_f<T<T_v$ would then be a phase with 2D correlations, which is in between the metallic and 3D superconducting phases; this phase was proposed by Friedel[27] to account for the observed power-law I-V relations.

A discrete-Gaussian version of the free energy (3) was studied by Korshunov,[28] showing that in fact $T_v<T_f$ for all parameters in the free energy. Korshunov's solution is equivalent to a first-order RG, which from Eq. (21) and Eq. (45) (with $J=0$) confirms that $T_v<T_f$ for all values of d/λ_e. In particular, for $d/\lambda_e \ll 1$, the ratio T/τ varies by a factor of 8 between $T=T_v$ and $T=T_f$. The effect of the second-order RG, for $d/\lambda_e \ll 1$, is to lower T_v and enhance T_f, so that $T_v<T_f$ is still valid. For $\lambda_e/d \lesssim 1$, the presence of the finite-size transition T_v^{eff} can change the situation, as discussed below.

For $d/\lambda_e \ll 1$, the separate vortex and fluxon study is inconsistent and an intermediate 2D phase does not exist. The only general statement is that for $T>T_f$, where $J\to 0$, it is consistent to have free vortices, i.e., a normal phase, while, for $T<T_v$ with no vortices, it is consistent to have a finite renormalized J, i.e., a 3D superconducting phase with long-range order. The phase transition between these phases is therefore a single 3D transition at a temperature T_c which is in the range $T_v<T_c<T_f$.

I proceed now to determine T_c by comparing the correlation lengths ξ_v and ξ_f. Interpreting ξ_v^{-2} as the mean density of vortices (Appendix B), vortices are absent in the cosine term of (15) on a scale $\xi<\xi_v$ and the scaling of the fluxon system is valid up to $\min(\xi_v,\xi_f)$. Now, if $\xi_f<\xi_v$, J is normalized to strong coupling on a scale shorter than ξ_v and vortices are not available to interfere with the fluxon scaling. A strong J implies an isotropic system, so that $\xi_f<\xi_v$ is a sufficient condition for a 3D ordered phase. On the other hand, if $\xi_v<\xi_f$, vortices on a scale ξ_v interfere in the cosine term of (15) and prevent J from being fully renormalized. The system remains anisotropic and disordered; hence, the criterion for T_c is $\xi_v \approx \xi_f$. This criterion determines the highest temperature at which the system scales into an isotropic one, which must be an ordered phase since $T<T_c^0$. The criterion $\xi_v \approx \xi_f$ incorporates 2D fluctuations due to anisotropy, but ignores the final "fine-tuning" due to 3D-type fluctuations.

A geometric interpretation can be given, based on the identification of ξ_f as a typical size of the fluctuating fluxon loop. The criterion $\xi_v \approx \xi_f$ means then that the in-layer vortex spacing matches the size of the fluxon loops so that they can efficiently combine to from 3D vortex loops, as needed in a 3D fluctuation regime.

The implication of the criterion $\xi_v \approx \xi_f$ is illustrated in Fig. 5 for systems with $\lambda_e/d \gg 1$. The dashed lines represent scaling of the vortex fugacity, while the solid lines represent those of the Josephson coupling; note the opposite direction of the flow of the effective temperature and the locations of T_v and T_f. In particular, the two trajectories near T_c/τ correspond to the condition $\xi_v \approx \xi_f$; the vortex scaling is assumed to start from a smaller y_0 than the corresponding J/T for the fluxon system. Thus, in order to reach the same ξ when y scales to ≈ 1, the vortex system must scale faster than the fluxon system, which is possible if T_c is closer to T_f than to T_v.

Note that if the renormalization of ξ_f by v and by T/τ is neglected [$T/\tau \ll 1$ in Eq. (47)], the criterion $\xi_v \approx \xi_f$ becomes that of Ref. 29; i.e., the interlayer coupling in area ξ_v^2 satisfies $J\xi_v^2/\xi_0^2 \approx T$; this obviously misses the effect of T_f on the transition, as well as a renormalization of ξ_v by J (see below), effect which, as shown below, are negligible only when J/T is exponentially small.

Before applying the criterion $\xi_v \approx \xi_f$, the definition of ξ_v must be reconsidered. The fluxon scaling [e.g. Eq. (52) if T is not too close to T_f] is valid for $\xi < \min(\xi_v, \xi_f)$. In contrast, the vortex scaling [e.g., Eq. (37) for T not too close to T_v] is never correct for $J \neq 0$ since nonlinearity due to vortices is present in both their direct interaction [first term of Eq. (15)] and in the cosine term of Eq. (15). This asymmetry is related to the fact that Eq. (15) is not self-dual; i.e., performing the transformation of Eq. (28) on the full system does not lead to a system similar to itself.

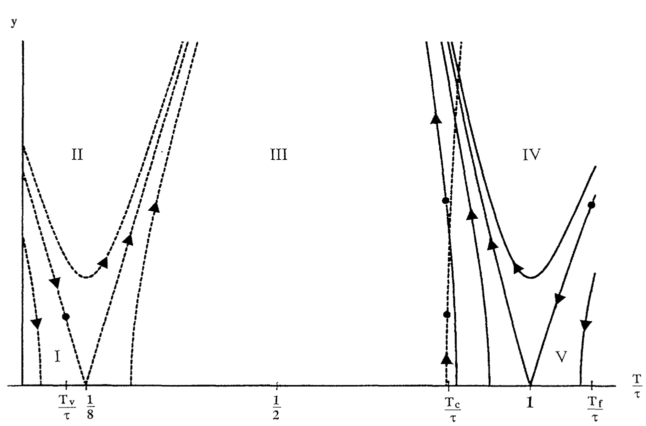

FIG. 5. Schematic scaling trajectories of vortex fugacity (dashed lines) and Josephson coupling (solid lines) for $d \ll \lambda_e$. The axis T/τ is here a renormalized temperature, i.e., $h_0 + T/\tau$ for the vortex system and $[h_0 + \tau/T]^{-1}$ for the fluxon system. In region I vortex fugacity is irrelevant and Josephson coupling is relevant; region V has the opposite behavior. In regions II, III, and IV both vortex fugacity and Josephson coupling are relevant. Regions II and IV correspond to the behavior of Eqs. (36) and (46), respectively, while the wide region III corresponds to Eqs. (53) and (55). Solid circles mark the initial values on the trajectories defining T_v and T_f and on the crossing trajectories (for which $\xi_v \approx \xi_f$) which determine T_c.

To find ξ_v, I construct a variational free-energy density $f(\xi_v)$, which includes, in addition to the usual interaction and entropy terms[38] (see Appendix B), the free-energy gain from integrating the J^2 and v^2 terms [Eq. (A19)]. The fluxon terms (A19) can be integrated up to ξ_v (with $\xi_v < \xi_f$ in mind), which together with the vortex free energy (B6) yields an effective free-energy density

$$f(\xi_v) = \{(T - \tau/8)\ln[\xi_0^2/e\xi_v^2] + E_c - T\ln 2\}/[b(T)\xi_v^2] - \gamma' T \int_{\xi_0}^{\xi_v} [\tfrac{1}{2}X_0 \bar{J}^2(\xi) + (X_0 + X_1)v^2(\xi)]\xi^{-3} d\xi \ , \tag{54}$$

where $\bar{J}$ (y of the fluxon system) is the renormalized J/T, X_0 and X_1 are ξ dependent from Eq. (41), and $b(T)$ is given by Eq. (B5). The vortex correlation length ξ_v is found by minimizing (54), leading to the form (37), but with a renormalized E_c', i.e.,

$$\xi_v \approx \xi_0 \exp[\tfrac{1}{2}E_c'/(T - \tau/8)] \ , \tag{55}$$

where, with $X_0 \approx -2X_1 \approx T/\tau$ for simplicity [Eq. (42)],

$$E_c' = E_c - T\ln 2 + \tfrac{1}{8}\gamma' b(T)(T^2/\tau)[\bar{J}^2(\xi_v) + v^2(\xi_v)] \ . \tag{56}$$

Thus E_c' is enhanced by the Josephson term; for determining T_c, we need $\xi_v \approx \xi_f$ in Eq. (56) so that $\bar{J}^2(\xi_v) \approx 1$ and $v^2(\xi_v) \lesssim 1$.

The criterion $\xi_v \approx \xi_f$ can now be applied. Consider first the two extreme regions II and IV of Fig. 5. In region II, very near T_v, Eqs. (36) and (47) should be used with the result

$$T_c - T_v \sim [\ln(T_c/J)]^{-2} \ , \tag{57}$$

in agreement with Ref. 29, but differing from the suggestion of Ref. 28. In the other extreme of region IV, very near T_f, Eqs. (46) and (55) could be used. A solution for $T_c/\tau > 1$ is possible if $\tilde{\gamma}J/T > T/E_c'$; i.e., a large core energy is required [including the effect of the v term on Eq. (46) should effectively enhance J in the inequality]. The result for T_f in terms of τ_0 is

$$T_f - T_c \approx 0.1 T_f^5/(\tilde{\gamma} J E_c'^2 \tau_0) \ . \tag{58}$$

Most of the possible variation of T_c is in the wide region III of Fig. 5; equating Eqs. (55) and Eq. (53) yields, for this region,

$$T_c \approx \tau \frac{\eta E_c' + \frac{1}{8}\tau \ln T_c/J}{\eta E_c' + \tau \ln T_c/J} \ . \tag{59}$$

To allow for T_c in regions where second order RG is significant, the equation $\xi_v(T) = \xi_f(T)$ is solved numerically for $T = T_c$, as shown in Fig. 6; ξ_v is the scale at which the solution of Eq. (31) reaches $\gamma y = 1$ and similarly for ξ_f by solving Eq. (A20) with Eq. (41). [The renormalization $E_c \to E_c'$ of Eq. (56), which is neglected in Fig. 6, would make the curves of Fig. 6 steeper at $T_c/\tau \gtrsim 1$]. For a small E_c/τ (≈ 0.5) the results of the conventional X-Y model are reproduced, i.e., T_c/τ changes by a factor of ≈ 2. For larger E_c/τ the variation in T_c/τ increases and $T_c > \tau$ is possible, i.e., T_c/τ changes by $\gtrsim 8$. The

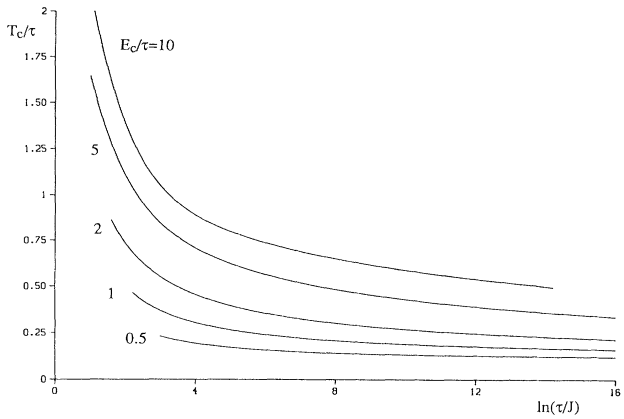

FIG. 6. 3D transition temperature T_c as obtained by solving second order RG for $\xi_v(T)=\xi_f(T)$ with $\lambda_e/d=10^6$, $d/\xi_0=1$, $\gamma=\gamma'=4$ and values of E_c/τ as indicated. Other choices of γ,γ' [Eq. (A7)] lead to approximately the same curves if J in the abcissa is replaced by $\gamma J/4$.

range for T_c/τ variation is therefore a sensitive function of E_c/τ.

Conventional calculations of E_c are based on an amplitude-dependent Ginzburg-Landau theory,[39,40] leading to $E_c/\tau=0.2$ (Ref. 39) and to $E_c/\tau=0.12$ [Ref. 40 for Eq. (27)]. However, in view of the short coherence length of CuO_2-based superconductors, the required amplitude variation is too fast and a microscopic derivation is necessary. It is safer then to consider E_c in the starting free energy (3) as a parameter, to be determined by experiment.

It is worth mentioning that when fluctuations are ignored E_c can be absorbed into the definition of ξ_0; e.g., the energy of a vortex pair is

$$(\tau/2)\ln r/\xi_0+2E_c=(\tau/2)\ln r/\xi^{\text{eff}} .$$

However, including thermal fluctuations shows that E_c and ξ_0 are independent parameters; i.e., scaling between ξ^{eff} and ξ_0 is not equivalent to eliminating E_c. Thus ξ_0 is considered here as the cutoff on phase fluctuations, while the core energy E_c is a term in the vortex energy, which is *in addition* to phase-dependent energies and is therefore independent of ξ_0.

Several of the layered compounds show[12-14] a resistivity of the form (1), which allows an estimate of E_c. This resistivity is related to ξ_v via Eq. (36), and the parameter b in Eq. (1) is then related to $y_0=2\exp(-E_c/T)$ in Eq. (36). The experimental fits to Eq. (1) for[12] $Bi_2Sr_2CaCu_2O_x$ and for[13] $Tl_2Ba_2CaCu_2O_8$ yield $E_c/\tau=0.4+\frac{1}{8}\ln\gamma$, while for[14] $YBa_2Cu_3O_7/PrBa_2Cu_3O_7$ superlattices $E_c/\tau=0.5+\frac{1}{8}\ln\gamma$. In view of the nonuniversal parameter γ and the renormalizations in E_c' [Eq. (56)] and η [Eq. (52)], the factor $\eta E_c'/\tau$ in (59) may well be above 1.

Finally, the situation for $\lambda_e/d<1$ is considered. As shown in Sec. III, there is a finite-size transition $T_v^{\text{eff}}\approx\tau/8$ [Eq. (38)], which is not sensitive to λ_e/d. In contrast, $T_f\sim 2\lambda_e\tau/d$ [Eq. (45)] so that a situation with $T_f<T_v^{\text{eff}}$ can be achieved allowing for an intermediate 2D phase. This situation is relevant to 2D junctions between bulk superconductors—as discussed below Eq. (38), $T_v^{\text{eff}}\to T_c^0$, while T_f is decreasing like $1/d$ [T_f formally vanishes as $d\to\infty$; however, modifying the model Eq. (3) for this case[26] leads to a finite T_f].

The latter result is remarkable: A boundary such as a junction can be thermally disordered, while the bulk has long-range order. This result is due to $e\neq 0$—the finite screening length λ_e allows fluxon fluctuations in the junction, while the bulk remains ordered. For the *X-Y* model, $\lambda_e\sim e^{-2}\to\infty$ and the junction orders as soon as the bulk does.

VI. DISCUSSION

The main relevant result of the present work to experiment is the allowed range of T_c as J varies from 0 (when $T_c\to T_v$) to the strong coupling of the isotropic system. Section V shows that the vortex-core energy, or its renormalized version $\eta E_c'$ in Eq. (59), has a significant effect on the possible range of T_c/τ. For $\eta E_c'\lesssim\tau$, the results are consistent with the conventional *X-Y* model[30,31] where T_c/τ varies by a factor of 2.4. However, when E_c' is moderately large, so that $\exp(-\eta E_c'/\tau)\ll 1$, T_c/τ can vary by a larger factor of up to 8. When E_c' is even larger, i.e., $E_c'\gg T_c$, the variation in T_c/τ can be even larger than 8 [Eq. (58)].

Note that a given variation of T_c/τ implies a much smaller variation in an actually measured T_c, since τ is T dependent. Assuming the form $\lambda_{ab}=\lambda'(1-T/T_c^0)^{-1/2}$ and $\lambda_{ab}^2=\lambda^2 d/d_0$, as discussed below Eq. (27), yields $\tau=\tau_0(1-T/T_c^0)$, where $\tau_0=\phi_0^2 d/(4\pi^2\lambda'^2)$; for the CuO_2-based superconductors (excluding superlattices), typically $\tau_0\approx 10^4$ K (see Table I of Ref. 16). Defining α as the variation in T_c/τ, i.e., $T_c=\tau/8$ when $J\to 0$ and $T_c=\alpha\tau/8$ when J is large, yields T_c in the range

$$T_c^0/(1+8T_c^0/\tau_0)<T_c<T_c^0/(1+8T_c^0/\alpha\tau_0) . \qquad (60)$$

Since $T_c^0\ll\tau_0$, the variation in T_c/T_c^0 is fairly small.

The Josephson coupling can be estimated by the anisotropy as defined below Eq. (4), and experimental data.[41] Using $\xi_0\approx d$ and $\tau_0\approx 10^4$ K yields, for $YBa_2Cu_3O_7$, $J\approx 10$ K (with an anisotropy of 5^2), while, for $Bi_2Sr_2CaCu_2O_8$, $J=0.1$ K (with an anisotropy of 55^2). Thus even in the latter case $\ln(T_c/J)\approx 7$ is not large in the sense that, for $\eta E_c'\gtrsim\tau$, T_c is still much larger than T_v.

Experimental data on $(YBa_2Cu_3O_7)_m(PrBa_2Cu_3O_6)_n$ superlattices[2-4] show a significant reduction in T_c with increasing n. Consider first the large-n data ($n=16$) where T_c is near T_v; the results of the sharper transitions[4] of $n=16$ with $m=3$, 4, and 8 can be fitted with the left-hand side of (60) using $T_c^0\approx 92$ K and $\tau_0/m=1200$ K$\pm$30%. This implies that λ_{ab} is somewhat larger than in bulk $YBa_2Cu_3O_7$; i.e., there is some loss of electron condensate.[32] In fact, nonlinear *I-V* data[14] on the $m=2$, $n=8$ and $m=4$, $n=8$ compounds has shown a reduction in T_c^0, implying a change in intralayer parameters. It is therefore essential to measure intralayer properties directly, in particular λ_{ab}, which can allow a separation of the contributions to the T_c reduction from either a change in intralayer parameters or from 2D fluctuations.

The Josephson coupling is expected to change as $\ln J \sim d$, where $d \sim n$ increases with the $PrBa_2Cu_3O_7$ thickness. Figure 6 can therefore be compared with experimental data on $T_c(n)$ [more precisely, T_c/T_c^0 should be plotted rather than T_c/τ; the T_c/T_c^0 plot is, however, similar to that of Fig. 6, except that the overall scale is reduced to that of Eq. (60)]. Indeed, the initial fast reduction and the eventual saturation[3,4] in $T_c(n)$ is consistent with Fig. 6 with the parameter E_c/τ determined mainly by the overall change in T_c. Experimentally, T_c changes by a large factor; e.g., the $m=1$ compound changes from $T_c=90$ K ($n=0$) to $T_c \approx 20$ K ($n=16$). For a small α such as 2.4, the range in Eq. (60) is extremely small; if a reasonable fraction of the T_c reduction is due to 2D fluctuations (as implied by the saturation at high n), it would imply a larger value of α. Further data on λ_{ab} are again essential for settling this issue.

Data on the more anisotropic systems $(Bi_2Sr_2CaCu_2O_8)_m(Bi_2Sr_2CuO_6)_n$ have shown a decrease of T_c from 59 K ($n=0$) to ~ 30 K ($m=1$, $n=2$) with $Bi_2Sr_2CuO_6$ being a semiconductor.[6] Similar superlattices[7] showed no change in $T_c=75$ K from $n=0$ to $m=1$, $n=5$; however, $Bi_2Sr_2CuO_6$ in the latter case is a superconductor with $T_c=15$ K and is therefore less effective in decoupling the $Bi_2Sr_2CaCu_2O_8$ layers. Furthermore, iodine intercalation of $Bi_2Sr_2CaCu_2O_x$ shows that T_c is reduced by 10 K, although the crystal sheet resistance is hardly affected by the intercalation.[8] This indicates that intralayer properties are weakly affected, leaving the change in interplane coupling as the main cause for the reduction T_c. Thus, even for the small-J system of $Bi_2Sr_2CaCu_2O_8$, a further decrease of J by forming a superlattice or by intercalation seems to reduce T_c, in agreement with the theoretical estimate presented above.

The separate studies of the vortex and fluxon systems lead to further interesting results. The vortex system (Sec. III) shows that a system with $\lambda_e \ll d$ has a finite-size transition T_v^{eff} at a much higher temperature than T_v. This leads to the possibility of 2D phases on well-separated junctions. The fluxon system (Sec. IV) shows that for $\lambda_e \gg d$ a significant Josephson coupling between next-nearest layers is generated. Thus the relevance of the fluxon description can be tested experimentally, e.g., by a strong second harmonic in the ac Josephson effect.

A related set of experiments involves the observation of power-law I-V relations in a number of layered superconductors.[12–15] This behavior indicates 2D fluctuations and needs therefore to be reconciled with the presence of a finite-interlayer Josephson coupling. In the subsequent work[16] I study the effect of magnetic fields parallel to the layers and show that 2D behavior is in fact possible with a relatively strong Josephson coupling.

To conclude, the present work has gained insight into the nature of phase transitions in anisotropic systems with competing topological excitations. Experimental data on T_c of superlattices can be understood in terms of the competing vortex and fluxon phase transitions. It is hoped that further experimental data on these superlattices can separate the role of 2D fluctuations from changes in intralayer parameters and allow for a critical test of the present theory.

ACKNOWLEDGMENTS

I am grateful to A.I. Larkin, S. E. Korshunov, S. N. Artemenko, D. Baeriswyl, L. Bulaevskii, and D. C. Mattis for most valuable discussions. I thank the Institute for Scientific Interchange in Villa Gualino, Tornio, for their hospitality while part of this work was done. This research was supported by the Basic Research Foundation administered by the Israel Academy of Sciences and Humanities.

APPENDIX A: RG PROCEDURE

This appendix describes the RG procedure for a 3D sine-Gordon-type system which is critical only in 2D. The procedure is a momentum shell integration method, similar to that in 2D.[35–37] The formulation here is sufficiently general to apply for both the vortex and fluxon transitions.

Consider a partition function of the form

$$Z=\int \mathcal{D}\tilde{\chi}\exp\left[-\tfrac{1}{2}\int\frac{d^2q\,dk}{(2\pi)^3}G^{-1}(q,k)|\tilde{\chi}(\mathbf{q},k)|^2+\int\frac{d^2r}{\xi^2}\{y\cos[\tilde{\chi}_n(\mathbf{r})]+v\cos[\tilde{\chi}_n(\mathbf{r})+\tilde{\chi}_{n+1}(\mathbf{r})]\}\right], \tag{A1}$$

where $\mathbf{q},k$ are Fourier transform variables of r,n, respectively, and the q integration is cut off by $1/R<q<\Lambda$ ($\Lambda \approx 1/\xi$), while $|k|<\pi/d$. The v term is included as it turns out to be relevant for the fluxon system.

It is given that $G(q,k)$ is singular in q, but not in k, i.e., $G(q\to 0,\,k\neq 0)\sim q^{-2}$, while $G(q\neq 0,\,k\to 0)$ is finite. The $q=k=0$ result may depend on the order of limits, as is the case for the vortex transition; this does not affect the RG since the k integrations which follow are not sensitive to a single point.

The $\tilde{\chi}_n(\mathbf{r})$ is decomposed into a field $\chi_n(\mathbf{r})$ with Fourier components $q<\Lambda-d\Lambda$ and a field $\zeta_n(\mathbf{r})$ with Fourier components in the shell $\Lambda-d\Lambda<q<\Lambda$.

$$\tilde{\chi}_n(\mathbf{r})=\chi_n(\mathbf{r})+\zeta_n(\mathbf{r})\ . \tag{A2}$$

Consider the correlation function (integral limits indicated on $q=|\mathbf{q}|$ only)

$$G_\zeta(\mathbf{r},n)=\langle\zeta_n(r)\zeta_0(0)\rangle_\zeta = \int_{\Lambda-d\Lambda}^{\Lambda}\frac{d^2q\,dk}{(2\pi)^3}G(q,k)\exp(-i\mathbf{q}\cdot\mathbf{r}-iknd)\ , \tag{A3}$$

where $\langle \cdots \rangle_\zeta$ is an average with the Gaussian weight

$$\exp\left\{-\frac{1}{2}\int \frac{d^2q\,dk}{(2\pi)^3} G^{-1}(q,k)|\zeta(\mathbf{q},k)|^2\right\} .$$

Define

$$G^{-1}(q,k)=q^2\left[\frac{1}{g(q,k)}+h_0+h_1\cos kd\right]\Big/(8\pi d), \quad \text{(A4)}$$

with $g(q,k)$ nonsingular for either $q\to 0$ or $k\to 0$ and h_0,h_1 are two types of self-energies (as generated below by the RG) which are q and k independent. Performing the angular integral in (A3) yields

$$G_\zeta(\mathbf{r},n)=4d\int_{\Lambda-d\Lambda}^{\Lambda} dq\frac{J_0(qr)}{q}\int\frac{dk}{2\pi}\frac{g(q,k)}{1+(h_0+h_1\cos kd)g(q,k)}e^{-iknd} . \quad \text{(A5)}$$

In this form, $G_\zeta(\mathbf{r},n)$ has poor convergence at large r, a feature due to the sharp cutoff procedure.[35–37] In a smooth cutoff procedure, one replaces[36,37] the cutoffs by a smooth function, e.g., a mass insertion,

$$J_0(\Lambda r)d\Lambda/\Lambda\to\int_0^\infty dq\,qJ_0(qr)\left[\frac{1}{q^2+(\Lambda-d\Lambda)^2}-\frac{1}{q^2+\Lambda^2}\right]=rK_1(\Lambda r)d\Lambda , \quad \text{(A6)}$$

where $K_1(\Lambda r)$ is the Bessel function of imaginary argument. To first order in y, one needs only the $r=0$ value (see below) and then (A6) is an identity. To second order in y, one needs the averages

$$\int d^2\rho\,\rho^2J_0(\Lambda\rho)\to\gamma^2/(2\pi\Lambda^4),\quad \int d^2\rho\,J_0(\Lambda\rho)\to\gamma'/2\Lambda^2 . \quad \text{(A7)}$$

These integrals are formally divergent, but the replacement (A6) gives $\gamma=\gamma'=8\pi$; other smoothing functions yield different γ and γ'; i.e., γ,γ' are nonuniversal parameters. (If $\Lambda\xi$ is chosen as $\neq 1$, this can also be absorbed into the definition of γ and γ'.)

The RG proceeds by integrating out the field $\zeta_n(r)$. Rewrite (A1) as

$$Z=\int\mathcal{D}\chi\exp\left\{-\frac{1}{2}\int\frac{d^2q\,dk}{(2\pi)^3}G^{-1}(q,k)|\chi(\mathbf{q},k)|^2\right\}Z'\{\chi\}Z_0\{\zeta\} , \quad \text{(A8)}$$

with the normalization

$$Z_0\{\zeta\}=\int\mathcal{D}\zeta\exp\left\{-\frac{1}{2}\int\frac{d^2q\,dk}{(2\pi)^3}G^{-1}(q,k)|\zeta(\mathbf{q},k)|^2\right\} , \quad \text{(A9)}$$

so that an expansion to second order in y and v has the form

$$\begin{aligned} Z'\{\chi\}&=\left\langle \exp\left\{\sum_{n,\mathbf{r}}\{y\cos[\chi_n(\mathbf{r})+\zeta_n(\mathbf{r})]+v\cos[\chi_n(\mathbf{r})+\chi_{n+1}(\mathbf{r})+\zeta_n(\mathbf{r})+\zeta_{n+1}(\mathbf{r})]\}\right\}\right\rangle_\zeta \\ &=\exp[yI_1+vI_2+\tfrac{1}{2}y^2I_3+yvI_4+\tfrac{1}{2}v^2I_5+\cdots] . \end{aligned} \quad \text{(A10)}$$

Transforming the sum $\sum_{\mathbf{r}}$ to a sum $\sum'_{\mathbf{r}}$ of a lattice with $(1-d\Lambda/\Lambda)^2$ less degrees of freedom and using

$$\langle\exp[i\zeta_n(r)]\rangle_\zeta=\exp[-G_\zeta(0,0)/2]$$

yields, for small $d\Lambda$,

$$I_1=\left\langle\sum_{n,\mathbf{r}}\cos[\chi_n(\mathbf{r})+\zeta_n(\mathbf{r})]\right\rangle_\zeta=[1+2(d\Lambda/\Lambda)-\tfrac{1}{2}G_\zeta(0,0)]\sum_{n,\mathbf{r}}{}'\cos[\chi_n(\mathbf{r})] , \quad \text{(A11)}$$

$$\begin{aligned} I_2&=\left\langle\sum_{n,\mathbf{r}}\cos[\chi_n(\mathbf{r})+\chi_{n+1}(\mathbf{r})+\zeta_n(\mathbf{r})+\zeta_{n+1}(\mathbf{r})]\right\rangle_\zeta \\ &=[1+2(d\Lambda/\Lambda)-G_\zeta(0,0)-G_\zeta(0,1)]\sum_{n,\mathbf{r}}{}'\cos[\chi_n(\mathbf{r})+\chi_{n+1}(\mathbf{r})] , \end{aligned} \quad \text{(A12)}$$

$$\begin{aligned} I_3&=\left\langle\sum_{n,\mathbf{r}}\cos[\chi_n(\mathbf{r})+\zeta_n(\mathbf{r})]\sum_{n',\mathbf{r}'}\cos[\chi_{n'}(\mathbf{r}')+\zeta_{n'}(\mathbf{r}')]\right\rangle_\zeta-I_I^2 \\ &=\sum_{n,\mathbf{r}}\sum_{n',\mathbf{r}'}\tfrac{1}{2}G_\zeta(r-r',n-n')\{\cos[\chi_n(\mathbf{r})-\chi_{n'}(\mathbf{r}')]-\cos[\chi_n(\mathbf{r})+\chi_{n'}(\mathbf{r}')]\} . \end{aligned} \quad \text{(A13)}$$

In terms of $\rho=\mathbf{r}-\mathbf{r}'$ and $\mathbf{R}=\frac{1}{2}(\mathbf{r}+\mathbf{r}')$, $G_\zeta(\rho,n-n')$ is localized at $\rho\lesssim\Lambda^{-1}$ [see (A5) and (A6)] so that (A13) generates terms in the free energy of the form $\cos[\chi_n(\mathbf{r})-\chi_m(\mathbf{r})]$ $(n\neq m)$ or $\cos[\chi_n(\mathbf{r})+\chi_m(\mathbf{r})]$; all these terms; except possibly the v term, are assumed to be irrelevant; i.e., they renormalize to zero near the phase transition (the condition for this irrelevancy is obtained below). The only terms of I_3 which survive are $\cos[\chi_n(\mathbf{R}+\rho/2)-\chi_n(\mathbf{R}-\rho/2)]$ and the v term, which after expansion in ρ become

$$I_3=\frac{1}{2}\sum_{n,\mathbf{R}}\sum_{\rho}\{1-\tfrac{1}{4}\rho^2[\nabla\chi_n(\mathbf{R})]^2\}G_\zeta(\rho,0)-\tfrac{1}{2}\sum_{n,\mathbf{R}}\cos[\chi_n(R)+\chi_{n+1}(R)]\sum_{\rho}G_\zeta(\rho,1)+\text{irrelevant terms}\ . \tag{A14}$$

[In the vortex system, keeping the product form in Eq. (29) excludes $\rho=0$; this can be absorbed in the definition (A7) of γ'.] The gradient expansion neglects the higher-order terms in $\nabla\chi_n(R)$, which are also irrelevant as shown below. Considering next I_4, its only relevant term is $\cos\chi_n(\mathbf{r})$,

$$\begin{aligned}I_4&=\Big\langle\sum_{n,\mathbf{r}}\cos[\chi_n(\mathbf{r})+\zeta_n(\mathbf{r})]\sum_{n',\mathbf{r}'}\cos[\chi_{n'}(\mathbf{r}')+\chi_{n'+1}(\mathbf{r}')+\zeta_{n'}(\mathbf{r}')+\zeta_{n'+1}(\mathbf{r}')]\Big\rangle_\zeta-I_1I_2\\&=\sum_{n,\mathbf{r}'}\cos\chi_n(\mathbf{r}')\sum_{\rho}[G_\zeta(\rho,0)+G_\zeta(\rho,1)]+\text{irrelevant terms}\ .\end{aligned}\tag{A15}$$

The I_5 term generates, similar to I_2, gradient terms,

$$\begin{aligned}I_5&=\Big\langle\sum_{n,\mathbf{r}}\cos[\chi_n(\mathbf{r})+\chi_{n+1}(\mathbf{r})+\zeta_n(\mathbf{r})+\zeta_{n+1}(\mathbf{r})]\sum_{n',\mathbf{r}'}\cos[\chi_{n'}(\mathbf{r}')+\chi_{n'+1}(\mathbf{r}')+\zeta_{n'}(\mathbf{r}')+\zeta_{n'+1}(\mathbf{r}')]\Big\rangle_\zeta-I_2^2\\&=\tfrac{1}{2}\sum_{n,\mathbf{R}}\sum_{\rho}\{1-\tfrac{1}{4}\rho^2[\nabla\chi_n(\mathbf{R})+\nabla\chi_{n+1}(\mathbf{R})]^2\}\{2G_\zeta(\rho,0)+2G_\zeta(\rho,1)\}\ .\end{aligned}\tag{A16}$$

The Fourier transform of I_5 involves $1+\cos kd$ and hence the necessity of introducing the $h_1\cos kd$ term in Eq. (A4). The partition function becomes then, to second order in y and v,

$$\begin{aligned}Z=Z_0\int\mathcal{D}\chi\exp\Bigg\{&\frac{-1}{16\pi d}\int\frac{d^2q\,dk}{(2\pi)^3}q^2|\chi(\mathbf{q},k)|^2\left[\frac{1}{g(q,k)}+h_0+h_1\cos kd+2\gamma^2y^2X_0\frac{d\Lambda}{\Lambda}\right.\\&\left.\qquad+8\gamma^2v^2(X_0+X_1)(1+\cos kd)\frac{d\Lambda}{\Lambda}\right]\\&+\left[y\left[1+2\frac{d\Lambda}{\Lambda}-2X_0\frac{d\Lambda}{\Lambda}\right]+2\gamma'yv(X_0+X_1)\frac{d\Lambda}{\Lambda}\right]\sum_{n,\mathbf{r}}{}'\cos[\chi_n(\mathbf{r})]\\&+\left[v\left[1+2\frac{d\Lambda}{\Lambda}-4X_0\frac{d\Lambda}{\Lambda}-4X_1\frac{d\Lambda}{\Lambda}\right]-\tfrac{1}{2}\gamma'y^2X_1\frac{d\Lambda}{\Lambda}\right]\sum_{n,\mathbf{r}}{}'\cos[\chi_n(\mathbf{r})+\chi_{n+1}(\mathbf{r})]-dF/T\Bigg\}\ ,\end{aligned}\tag{A17}$$

where X_n are in general h_0, h_1, and Λ dependent,

$$X_n=d\int\frac{dk}{2\pi}\frac{g(\Lambda,k)\cos(nkd)}{1+(h_0+h_1\cos kd)g(\Lambda,k)}\ ,\tag{A18}$$

and dF is the free-energy contribution from the integrated $d\Lambda$ shell,

$$-dF/TV=\tfrac{1}{2}\gamma'y^2X_0\Lambda\,d\Lambda+\gamma'v^2(X_0+X_1)\Lambda\,d\Lambda+C\ ,\tag{A19}$$

where V is the volume and C a y-independent term due to (A9).

The final RG step is to rescale $q\to q'=q(1+d\Lambda/\Lambda)$ so that the original cutoff is recovered; one needs then to rescale

$$\chi(q,k)\to\tilde{\chi}(q',k)=\chi(q,k)(1-2d\Lambda/\Lambda)\ ;$$

this has the effect that $\chi_n(r)$ is replaced by $\tilde{\chi}_n(\mathbf{r}')$, as required to preserve the form of the cosine interaction. After this rescaling (A17) does not change, except that $g(q,k)$ is replaced by $g(q'/(1+d\Lambda/\Lambda),k)$.

The RG steps are now integrated from an initial cutoff Λ_0 to a final one Λ. The effect on $g(q,k)$ is to replace it by $g(q\Lambda/\Lambda_0,k)$; thus, all powers of q in $1/g(q,k)$ in (A17) scale to zero as $\Lambda\to0$—this is the reason for the standard claim that the higher-order terms in $\nabla\chi_n(R)$ are irrelevant. Second-order effects from y^2 or v^2 are neglected as the above rescaling is dominant for $g(q,k)$; note, however, that the q dependence of $g(q,k)$ can be significant via Eq. (A18).

Comparing (A17) with (A1) shows that the parameters y, v, h_0, h_1 are renormalized and become cutoff-dependent functions. Using ξ instead of Λ $(\xi\approx1/\Lambda)$ as the scaling variable, the recursion relations become

$$\begin{aligned}dy&=[2y(1-X_0)+2\gamma'yv(X_0+X_1)]d\ln\xi\ ,\\dv&=[2v(1-2X_0-2X_1)-\tfrac{1}{2}\gamma'y^2X_1]d\ln\xi\ ,\\dh_0&=[2\gamma^2y^2X_0+8\gamma^2v^2(X_0+X_1)]d\ln\xi\ ,\\dh_1&=8\gamma^2v^2(X_0+X_1)d\ln\xi\ .\end{aligned}\tag{A20}$$

These equations are to be integrated from an initial scale ξ_0 with initial conditions $y(\xi_0)=y_0$, $v(\xi_0)=v_0$, and $h_0(\xi_0)=h_1(\xi_0)=0$, which are the bare parameters in the starting free energy. To first order, there is a phase transition at $X_0=1$, assuming $X_1>-\frac{1}{2}$; for $X_0>1$, y is irrelevant ($d\ln y/d\ln\xi<0$), and for $X_0<1$, y is relevant ($d\ln y/d\ln\xi>0$). At a lower value of X_0, $X_0=\frac{1}{2}-X_1$, v becomes also relevant.

Finally, consider the condition for perturbations such as $w\cos[\tilde{\chi}_n(\mathbf{r})\pm\tilde{\chi}_{n'}(\mathbf{r})]$ to be irrelevant. To first order in w, renormalization involves

$$\left\langle \sum_{n,\mathbf{r}}\cos[\chi_n(\mathbf{r})\pm\chi_{n'}(\mathbf{r})+\zeta_n(\mathbf{r})\pm\zeta_{n'}(\mathbf{r})]\right\rangle_\zeta=[1+2(d\Lambda/\Lambda)-G_\zeta(0,0)\mp G_\zeta(0,n-n')]\sum_{n,\mathbf{r}}{}'\cos[\chi_n(\mathbf{r})\pm\chi_{n'}(\mathbf{r})]\ , \tag{A21}$$

for $n\neq n'$. Hence

$$dw=2w[1-2(X_0\pm X_{n-n'}]d\ln\xi\ . \tag{A22}$$

Near the phase transition $X_0=1$, the condition for irrelevancy is therefore

$$\pm X_{n-n'}>-\tfrac{1}{2}\quad(n\neq n')\ . \tag{A23}$$

For $n=n'$, $\cos 2\chi_n$ leads to $dw=2w(1-4X_0)d\ln\xi$, which is always irrelevant near $X_0=1$.

APPENDIX B: VORTEX FREE ENERGY

In this appendix a phenomenological effective free energy for a 2D vortex system is derived, following arguments of Young and Bohr.[38] This free energy involves adjustable parameters which are determined by the RG results.

The RG presented in Sec. III when $\lambda_e/d\gg1$ is, up to a minor shift in T_v, the same as that of a 2D vortex system; it involves the vortex fugacity y with the initial value $y_0=2\exp(-E_c/T)$ and v is irrelevant. When T is not too close to T_v [Eq. (35)], the first-order equation (33a) can be used with $X_0=\tau/8T$, leading to

$$y(\xi)=y_0\left[\frac{\xi}{\xi_0}\right]^{2(1-\tau/8T)}\ . \tag{B1}$$

The free energy per unit area due to vortex excitations is obtained by integrating Eq. (A19),

$$\begin{aligned}f_v&=-(\gamma'\tau/16)\int_{\xi_0}^{\xi_v}y^2(\xi)\xi^{-3}d\xi\\&=-(\gamma'\tau/32\xi_v^2)[1-y_0^{2(4T-\tau)/(8T-\tau)}]/(1-\tau/4T),\end{aligned} \tag{B2}$$

where ξ_v is determined by $y(\xi_v)\approx1$, leading to Eq. (37). Note that both terms in (B2) should be kept, to avoid a singularity[38] at $T=\tau/4$.

The phenomenological derivation of f_v assumes a vortex density n_v, proportional to ξ_v^{-2}. Since the mean spacing between vortices is $\sim n_v^{1/2}$, the logarithmic interaction energy per unit area is $n_v(\tau/4)\ln(\xi_0 n_v^{1/2})$ [Eq. (20a)], while the entropy is $\ln[(A/\xi_0)^{N_v}/N_v!]$, where A is the area and $N_v=An_v$. The free energy, as a variational function of n_v, has then the form

$$\tilde{f}(n_v)=(T-\tau/8)n_v\ln(\xi_0^2n_v)+n_vE_c(T)\ . \tag{B3}$$

This result shows, as is well known,[10,11] a phase transition at $T=\tau/8$; when $T<\tau/8$, $f(n_v)$ is a minimum at $n_v=0$, while at $T>\tau/8$ the minimum is at $n_v\neq0$. Defining $n_v=b^{-1}(T)\xi_v^{-2}$ yields two functions $E_c(T)$ and $b(T)$, which adjust the coefficients of the linear (n_v) and logarithmic ($\ln n_v$) terms. These coefficients are now determined by comparison with the RG results; n_v, which minimizes (B3) and Eq. (37), yield

$$E_c(T)=E_c-T\ln2+(T-\tau/8)\ln[b(T)/e]\ , \tag{B4}$$

while comparing the value of $f(n_v)$ at the minimum with Eq. (B2) yields

$$\begin{aligned}b(T)&=(4/\pi\tau)(T-\tau/8)(1-\tau/4T)\\&\quad\times[1-y_0^{(T-\tau/4)/(T-\tau/8)}]^{-1}\ .\end{aligned} \tag{B5}$$

At $T=\tau/8$, $b(T)$ vanishes and for $T>\tau/8$, it increases continuously to $b(T)\approx0.8$ at $T=\tau$. Substituting Eqs. (B4) and (B5) into Eq. (B3) yields for the effective free energy, written now in terms of ξ_v,

$$f(\xi_v)=b^{-1}(T)\xi_v^{-2}[(T-\tau/8)\ln(\xi_0^2/e\xi_v^2)+E_c-T\ln2]\ . \tag{B6}$$

This variational free energy has now the proper values at its minimum. Equation (B6) can now be used to study shifts from this minimum due to additional terms in the original free energy, as done in Sec. V.

[1] For a review on structure, see A. W. Hewat *et al.*, IBM J. Res. Dev. **33**, 220 (1989).

[2] J. M. Triscone, Ø. Fisher, O. Brunner, L. Antognazza, A. D. Kent, and M. G. Karkut, Phys. Rev. Lett. **64**, 804 (1990).

[3] Q. Li, X. X. Xi, X. D. Wu, A. Inam, S. Vadlamannati, W. L. Mclean, T. Venkatesan, R. Ramesh, D. M. Hwang, J. A. Martinez, and L. Nazar, Phys. Rev. Lett. **64**, 3086 (1990).

[4] D. H. Lowndes, D. P. Norton, and J. D. Budai, Phys. Rev. Lett. **65**, 1160 (1990).

[5] T. Terashima, K. Shimura, Y. Bando, Y. Matsuda, A. Fujiyama, and S. Komiyama, Phys. Rev. Lett. **67**, 1362 (1991).

[6] H. Furukawa, S. Tokunaga, and M. Nakao, Physica C **185-189**, 2083 (1991).

[7] I. Bozovic, J. N. Eckstein, M. E. Klausmeier-Brown, and G. F. Virshup, J. Superconduct. **5**, 19 (1992).

[8] X. D. Xiang, W. A. Vareka, A. Zettl, J. L. Corkill, M. L. Cohen, N. Kijima, and R. Gronsky, Phys. Rev. Lett. **68**, 530 (1992).

[9]B. I. Halperin and D. R. Nelson, J. Low Temp. Phys. **36**, 599 (1979).
[10]J. M. Kosterlitz and D. J. Thouless, J. Phys. C **6**, 1181 (1973).
[11]V. L. Berezinskii, Zh. Eksp. Teor. Fiz. **61**, 1144 (1971) [Sov. Phys. JETP **34**, 610 (1972)].
[12]S. N. Artemenko, I. G. Gorlova, and Yu. I. Latyshev, Phys. Lett. **138**, 428 (1989).
[13]D. H. Kim, A. M. Goldman, J. H. Kang, and R. T. Kampwirth, Phys. Rev. B **40**, 8834 (1989).
[14]S. Vadlamannati, Q. Li, T. Venkatesan, W. L. McLean, and P. Lindenfeld, Phys. Rev. B **44**, 7094 (1991).
[15]Q. Y. Ying and H. S. Kwok, Phys. Rev. B **42**, 2242 (1990).
[16]B. Horovitz, following paper, Phys. Rev. B **47**, 5964 (1993).
[17]W. E. Lawrence and S. Doniach, in *Proceedings of the Twelfth International Conference on Low Temperature Physics (LT-12),* Kyoto, 1970, edited by E. Kanda (Keigaku, Tokyo, 1971), p. 361.
[18]L. N. Bulaevskii, Usp. Fiz. Nauk. **116**, 449 (1975) [Sov. Phys. Usp. **18**, 514 (1976)].
[19]K. B. Efetov, Zh. Eksp. Teor. Fiz. **76**, 1781 (1979) [Sov. Phys. JETP **49**, 905 (1979)].
[20]M. V. Feigel'man, V. B. Geshkenbein, and A. I. Larkin, Physica C **167**, 177 (1990).
[21]S. N. Artemenko and A. N. Kruglov, Phys. Lett. A **143**, 485 (1990).
[22]A. Buzdin and D. Feinberg, J. Phys. (Paris) **51**, 1971 (1990).
[23]L. N. Bulaevskii, S. V. Meshkov, and D. Feinberg, Phys. Rev. B **43**, 3728 (1991).
[24]J. Clem, Phys. Rev. B **43**, 7837 (1991).
[25]B. Horovitz, Phys. Rev. B **45**, 12 632 (1992).
[26]D. Browne and B. Horovitz, Phys. Rev. Lett. **61**, 1259 (1988); B. Horovitz, Physica B **165-166**, 1109 (1990).
[27]J. Friedel, J. Phys. Condens. Matter **1**, 7757 (1989).
[28]S. E. Korshunov, Europhys. Lett. **11**, 757 (1990).
[29]S. Hikami and T. Tsuneto, Prog. Theor. Phys. **63**, 387 (1980).
[30]A. Schmidt and T. Schneider, Z. Phys. B **87**, 265 (1992).
[31]P. Minnhagen and P. Olsson, Phys. Rev. Lett. **68**, 3820 (1992).
[32]M. Rasolt, T. Edis, and Z. Tešanović, Phys. Rev. Lett. **66**, 2927 (1991).
[33]B. Horovitz, Phys. Rev. Lett. **67**, 378 (1991).
[34]J. Pearl, Appl. Phys. Lett. **5**, 65 (1964); in *Proceedings of the Ninth International Conference on Low Temperature Physics (LT-9),* edited by J. G. Daunt, D. O. Edouards, F. J. Milford, and M. Yaqub (Plenum, New York, 1965), p. 566.
[35]For a review, see J. Kogut, Rev. Mod. Phys. **51**, 696 (1979).
[36]T. Ohta and D. Jasnow, Phys. Rev. B **20**, 139 (1979).
[37]H. J. F. Knops and L. W. J. den Ouden, Physica **103A**, 597 (1980).
[38]A. P. Young and T. Bohr, J. Phys. C **14**, 2713 (1981).
[39]P. Minnhagen and M. Nylen, Phys. Rev. B **31**, 5768 (1985); P. Minnhagen, Rev. Mod. Phys. **59**, 1001 (1987).
[40]C.-R. Hu, Phys. Rev. B **6**, 1756 (1972).
[41]D. E. Farrell, S. Bonham, J. Forster, Y. C. Chang, P. Z. Jiang, K. G. Vandervoort, D. J. Lam, and V. G. Kogan, Phys. Rev. Lett. **63**, 782 (1989).